University of Nevada

Reno

Aftershocks of the May, 1980 Mammoth Lakes, California Earthquakes

A thesis submitted in partial fulfillment of the requirements

for the degree of Master of Science in Geophysics

by

Chester Scott Lide

December 1984

MINES
LIBRARY
Thesis
1920

The thesis of Chester Scott Lide is approved:

12/05/84

Thesis Advisor

12/5/84

Department Chairman

Dean, Graduate School

University of Nevada

Reno

December 1984

Acknowledgments

I would like to thank my thesis advisor, Dr. Alan Ryall for the guidance and encouragement which made this thesis possible. I wish also to thank the members of my thesis committee, Dr. Keith Priestley and Dr. William Cathey for their advice and guidance. Dr. Bill Peppin, Dr. Ed Corbett, Mr. Ron Sheen and Mr. David Chavez provided much of the computer software and gave helpful suggestions throughout the course of this research. Dr. Ute Vetter provided focal mechanisms used in this thesis. Flori Ryall and Gloria Smith were responsible for the analysis of much data used in this research. Wally Nicks and Austin Wilson deserve credit for the installation and operation of the equipment used in the acquisition of data. To all the staff at the Seismological Laboratory I express my sincere appreciation. Craig dePolo gave many helpful suggestions regarding the geology of Mammoth Lakes. Phil Sirles provided help in data acquisition and in the reproduction of this thesis. I thank Rob Cockerham for providing data from the USGS temporary stations and Mr. Roy Miller and the staff of the Seismographic Station, University of California, Berkeley for providing data from their network. Finally, I thank Kristy for putting up with the long hours during my years as a graduate student.

This research was partly supported by the U. S. Geological Survey under Contracts 14-08-0001-21248 and 14-08-0001-21863, and partly by the U. S. Department of Energy under Contract DE-AS08-82ER12082.

Abstract

Master-event relocation of aftershocks of the May, 1980 Mammoth Lakes earthquake sequence indicates a complex pattern of faulting in the mountains south of the Long Valley caldera. Locations of 344 aftershocks which occurred during the period 28 May to 30 July show two vertical NNE trends. These trends correspond well with nodal planes determined from short-period local and regional first-motions for many well located aftershocks indicating left-lateral strike-slip displacement on vertical faults is responsible for part of the seismicity. Numerous vertical fractures with this trend, some of which display left-lateral offsets, have been recognized in the southern epicentral area. The southwestern boundary of the aftershock zone is parallel to rangefront structures and is on strike with the Hartley Springs fault. This suggests that rangefront faulting extends south of the caldera and has played some role in the 1980 activity.

	Introduction	1
Chapter 1	Geological background	5
	Regional Tectonic Setting	5
	Geology	8
	Structure	13
	Summary	20
Chapter 2	Seismological Investigations	21
	Source Mechanisms	23
	Geodetic Measurements	29
	Spasmodic Tremor	31
	Attenuation of S-waves	31
	Crustal Structure	32
Chapter 3	Precise Locations of aftershocks	33
	Data Set	35
	Procedure	35
	Location Program	36
	Velocity Model	37
	Method	40
	Results	41
	Location of the ML 6 Events	49
	Effects of Station Distribution	51
	Discussion and Interpretation	51

Chapter 4	Seismicity in the Mono Basin-Excelsior Mountain Zone	57
	Introduction	57
	Geology	57
	Seismicity	58
	Discussion	60
	Summary	64
	References	65
Appendix A	List of Earthquakes	71

Introduction

Three ML 6 earthquakes on 25 May 1980 and a fourth ML 6 shock on 27 May 1980 occurred near Mammoth Lakes, California. These events were part of a major earthquake swarm which began in the fall of 1978 and has continued to the time of this writing. The earthquakes have occured along the southern boundary of the Long Valley caldera and beneath the high Sierra to the south. Long Valley caldera is a 17 km by 32 km elliptical depression formed .7 mybp, during the explosive eruption of the Bishop tuff.

The current sequence began with an ML 5.7 event on 4 October 1978, beneath the Wheeler Crest 30 km northwest of Bishop, California, and involved a northwesterly migration of activity into the vicinity of the ML 6 events of May 1980 (Ryall and Ryall, 1980).

The occurrence of the earthquakes adjacent to the caldera, observed uplift of the resurgent dome, outbreak of new fumarole activity in 1982, the existence of numerous young volcanic features, and the observation of several periods of localized and intense earthquake swarming caused the USGS to issue a volcanic hazard notice in May 1982.

The Mammoth Lakes sequence has been the focus of a considerable amount of scientific controversy (as well as confusion in the public media) of which the following is a brief outline.

Correlation of Epicenters and Faults

Little correlation of epicenters and mapped faults has been recognized. The locations of the ML 6 events are along the southern caldera boundry and beneath the mountains to the south. These locations are well to the west of the Hilton Creek fault, a NNW-striking NE-dipping normal fault that displays the most striking Holocene displacement of any fault in the area.

The Hilton Creek fault is often called the most important fault in the Mammoth Lakes area and has been suggested as the causative fault for the ML 6 events (Taylor and Bryant, 1980). Minor rupturing was observed on the Hilton Creek fault following the ML 6 events, while most of the additional surface rupture ocurred within Long Valley and consisted of predominantly normal and obliquc offsets on NW striking normal faults. With the exception of the southern caldera boundary, faults with the geometry inferred from epicenters and focal mechanisms have not been recognized in the vicinity of the ML 6 events.

Source Mechanisms

Considerable controversy has arisen over the P-wave radiation patterns and moment-tensor solutions for the largest events of the sequence. Discrepancies exist between mechanisms derived from local and regional first motion data and those derived from first motions and moment-tensor inversions for long-period teleseismic body and surface waves. Focal mechanisms for the mainshock derived from local and regional P-wave first motions yield strike-slip mechanisms on near vertical faults, either left-lateral on NNE faults or right-lateral on WNW striking faults (Cramer and Toppozada, 1980 ; Ryall and Ryall, 1981a). Long-period teleseismic P-wave first motions require oblique slip on a moderately dipping fault plane (Given *et al.* 1982; Barker and Langston, 1983) and opposite first motions for short and long period instruments have been observed for several stations at teleseismic distances (Wallace *et al.* 1982; Barker and Langston, 1983). Moment-tensor inversions for long-period body and surface waves yield solutions with large non-double couple components (Barker and Langston, 1983; Ekstrom and Dziewonski, 1983; Ekstrom, 1983; Julian, 1983;

Sipkin and Julian, 1983; Aki, 1984). Several workers (Julian, 1983; Sipkin and Julian, 1983; Aki, 1984) suggest that several of the large events were caused by dike injection (tensile rather than shear failure) based on combined local, regional and teleseismic first motions as well as moment-tensor inversion. Other workers have found it possible to model the first ML 6 event as a multiple rupture on a variety of different fault planes (Barker and Langston, 1983; Ekstrom, 1983; Wallace, 1983:1984). A change in mechanism, from dominantly strike-slip to dominantly oblique and normal slip with increasing depth, has been observed for well located aftershocks (Vetter and Ryall, 1983).

Geodetic data indicates uplift within the caldera between July 1979 and September 1980, centered on the resurgent dome (Savage and Clark, 1982). This uplift has been attributed to reinflation of a magma chamber and it has been suggested this may have caused or triggered the ML 6 events (Savage and Clark, 1982; Rundle and Whitcomb, 1983). There is, therefore, the suggestion that the Mammoth Lakes earthquakes were caused by volcanic processes rather than tectonic. There is much evidence for magmatic ativity in the area, but the question remains as to its relation to the seismicity.

This investigation focuses on master-event relocation of aftershocks of the May 1980 sequence for the period between 28 May and 30 July 1980. Chapter 1 is a summary of geologic work in the vicinity of Mammoth Lakes and presents data and observations by early workers which appear to be significant in understanding the seismic processes involved at Mammoth Lakes. Chapter 2 summarizes previous seismological and geophysical studies done for the area and for the 1980 earthquake sequence. Chapter 3 presents the method and results of precise master-event relocations of aftershocks of the May 1980 sequence.

The onset of the Mammoth Lakes seismicity in October 1978 was associated with a flare-up of activity along the entire Sierra Nevada-Great Basin Boundary Zone (SNGBZ; Ryall and Ryall, 1981a). Following the 1980 earthquakes, activity began to occur in the Adobe Hills area east of Mono Lake. This activity was observed to migrate to the northeast involving distinct clusters within the Mono Basin-Excelsior Mountain zone (MBEMZ), a zone of predominantly Left-lateral displacement on ENE striking faults (Gilbert *et al.* 1968). Focal mechanisms are in agreement with left-lateral strike-slip on ENE striking faults (Vetter and Ryall, 1983). Chapter 4 presents a discussion on the seismicity of the MBEMZ and evidence for migrating seismicity.

Chapter 1.

Geological Background

Physiography

The 1980 Mammoth Lakes earthquake sequence occurred along the eastern escarpment of the Sierra Nevada near the resort town of Mammoth Lakes, California. Mammoth Lakes is located in the southwestern portion of the Long Valley caldera. The caldera forms a large reentrant into the Sierra Nevada north of Owens Valley known as the "Mammoth Embayment." South of the caldera the mountains rise about 4000 feet and form a broad salient that extends east to the eastern slopes of McGee Mountain and Wheeler Crest. To the southeast is Round Valley and the town of Bishop which is located at the northern end of Owens Valley.

Regional Tectonic Setting

The Mammoth Lakes area is located on the eastern escarpment of the Sierra Nevada along the SNGBZ. This zone separates the Basin and Range Province, a region of active crustal extension characterized by a system of parallel horsts and grabens, thin crust, high heat flow, and relatively low gravity (Stewart, 1971; Thompson and Burke, 1974) from the Sierra Nevada, a relatively coherent block characterized by thick crust (Eaton, 1966) and low heat flow. Figure 1 shows the location of the Mammoth Lakes area in relation to the Sierra Nevada and western Great Basin along with seismicity for the period 1978-1983. The SNGBZ is a structurally complex zone exhibiting both strike-slip and normal faulting. The Walker Lane is a NW-trending zone characterized by right-lateral strike-slip and forms a boundary between NNW-trending structures to the west

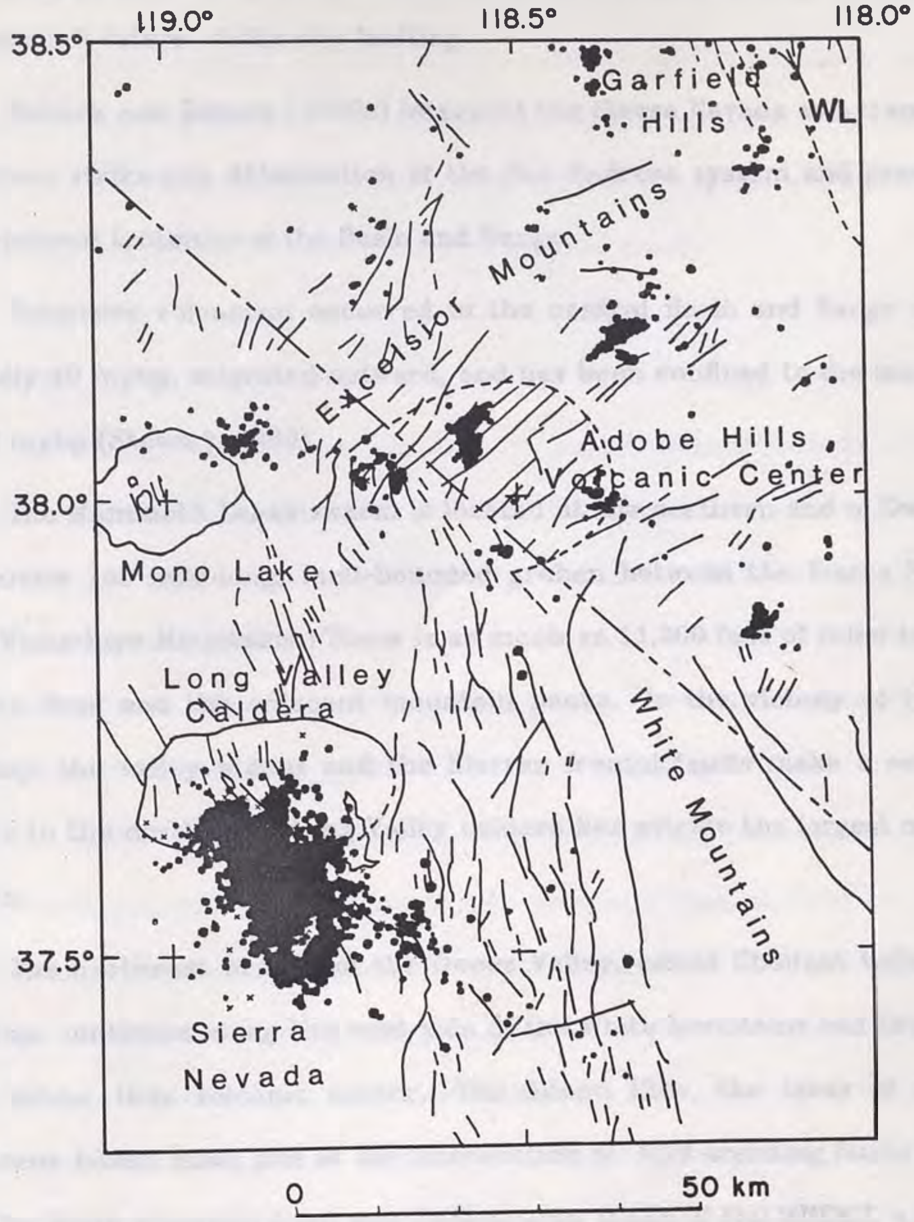

Figure 1. Map showing faults in the Mammoth Lakes/northern Owens Valley region and seismicity for the period 1978-1983. Faults taken from Strand (1967) and Stewart and Carlson (1978). WL – Walker Lane.

and NNE-trending structures to the east (Slemmons *et al.*, 1979; Bell and Slemmons, 1979). ENE-trending structures of the MBEMZ (Gilbert *et al.*, 1968) and the Olinghouse, Midas and Carson lineaments (Sanders and Slemmons, 1979) exhibit left-lateral strike-slip faulting.

Zoback and Zoback (1980a) interpret the Sierra Nevada as a transition zone between strike-slip deformation of the San Andreas system and predominantly extensional tectonics of the Basin and Range.

Extensive volcanism occurred in the central Basin and Range at approximately 40 mybp, migrated outward, and has been confined to the margins since 5-10 mybp (Stewart, 1980).

The Mammoth Lakes swarm is located at the northern end of Owens Valley, a narrow 150 mile-long, fault-bounded graben between the Sierra Nevada and the White-Inyo Mountains. There is as much as 11,000 feet of relief between the valley floor and the adjacent mountain peaks. In the vicinity of the town of Bishop, the valley widens and the Sierran frontal faults make a series of left steps to the northwest. Long Valley caldera lies astride the largest of those left steps.

The northeast branch of the Owens Valley, called Chalfant Valley north of Bishop, continues along the west side of the White Mountains and terminates at the Adobe Hills volcanic center. The Adobe Hills, the locus of voluminous Pliocene basalt flows, lies at the intersection of NNW-trending faults that parallel the White Mountain front and ENE-striking faults of the MBEMZ, a broad zone of left-lateral faulting (Gilbert, *et al.* 1968).

Three principle zones of faulting have been recognized in Owens Valley (Carver, 1970). These include two zones along the east and west sides of the valley, characterized by dominantly normal faulting, and a third zone of both normal and oblique faulting in the center of the valley.

Geodetic measurements in southern Owens Valley indicate that tectonic strain is essentially pure right-lateral tensor shear at a rate of 0.08 μstrain/a across a vertical plane trending N20W; however, north of Bishop the strain is nearly uniaxial extension in the N70E direction.(Savage *et al.* 1980). This results in right-lateral strike-slip parallel to the axis of the valley south of Bishop and spreading of the valley by normal faulting to the north.

Geology

The oldest rocks in the area are Paleozoic metasediments of the Mount Morrison roof pendant. Rinehart and Ross (1964) describe the roof pendant as a grossly homoclinal sequence of Paleozoic Metasediments with maximum stratigraphic thickness of 32,400 feet. Beds strike northwest and have steep dips with tops to the west. Mesozoic metavolcanic rocks occur in the western portion of the roof pendant and have a total thickness of about 13,600 feet.

The rocks of the Mount Morrison roof pendant are intruded by Jurassic and Cretaceous plutonic rocks of the Sierra Nevada Batholith, ranging in composition from granodiorite to quartz-monzonite. Figure 2 is a geologic map after Rinehart and Ross (1964) showing the plutonic and metamorphic rocks south of the caldera. Several of the plutonic contacts are linear and have strikes in directions which are locally expressed in the rangefront. Similar observations by Mayo (1941) led him to suggest that the rangefront faults are locally controlled by an older structural framework. Plutonic contacts are typically sharp and some exhibit catacastic textures suggesting emplacement in a brittle or semi-brittle state.

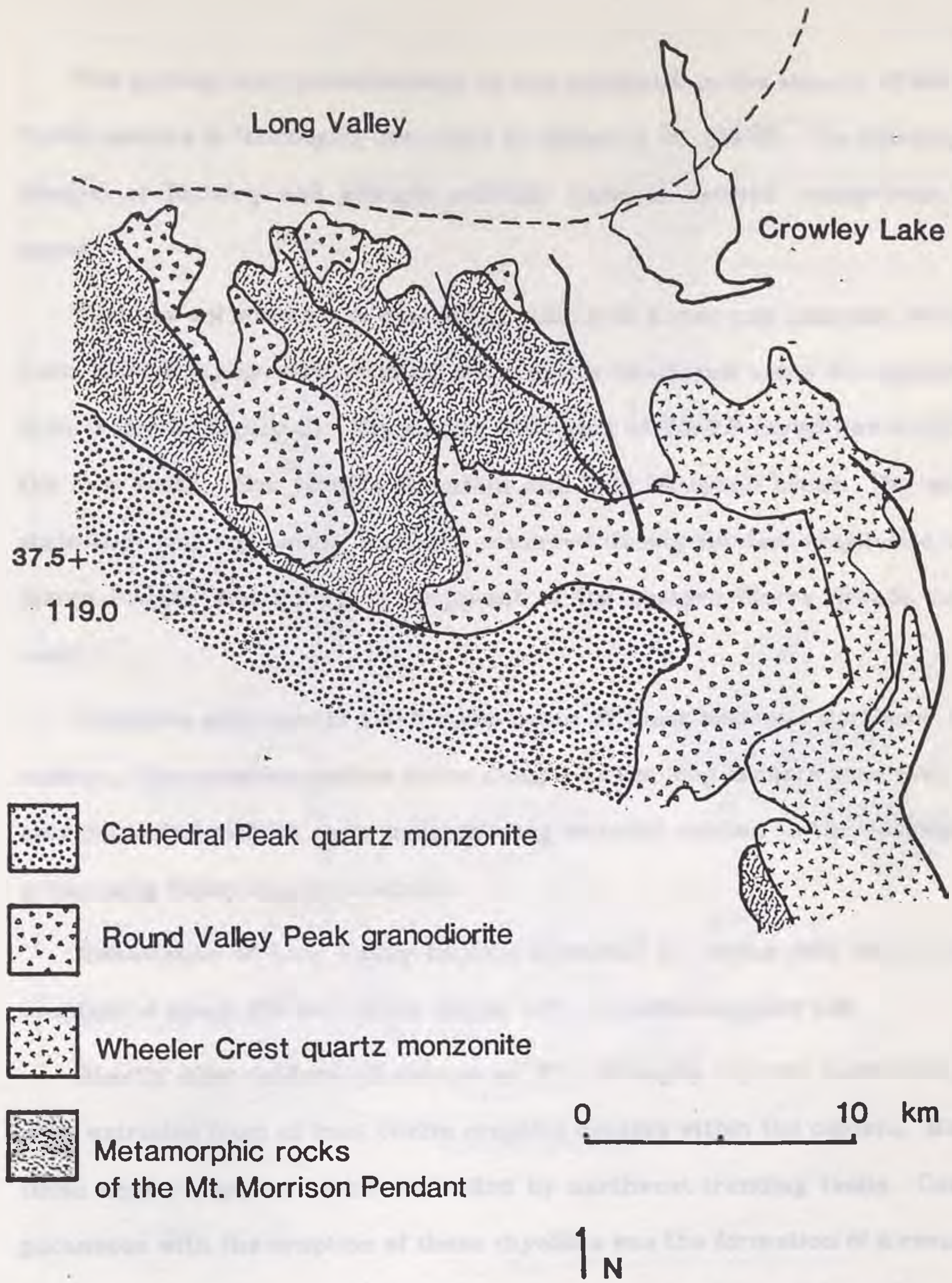

Figure 2. Geologic map after Rinehart and Ross (1964) showing plutonic and metamorphic rocks in the epicentral area.

The geology and geochronology of the volcanism in the vicinity of the Long Valley caldera is thoroughly discussed by Bailey *et al.* (1976). The following discussion of Tertiary and younger volcanic rocks is derived chiefly from their paper.

Tertiary volcanic rocks consisting mainly of basalt and andesite with ages from 3.2-2.6 mybp were erupted from widely scattered vents throughout the area (refer to Figure 3). Rhyodacite with ages of 3.2-2.7 mybp was erupted in the Two Teats - San Joaquin Mountain and Bald Mountain areas. The authors state that this volcanism "probably occurred during the last major rise of the Sierra Nevada and before development of the eastern Sierra Nevada escarpment."

Rhyolites with ages of 1.9-.9 mybp occur at Glass Mountain northeast of the caldera. The eruptive centers occur along a 13 km long arcuate zone that probably coincides with an early incipient ring fracture related to the development of the Long Valley magma chamber.

Subsidence of Long Valley caldera occurred 0.7 mybp with the explosive eruption of about 600 km^3 of the Bishop tuff, a rhyolite ash-flow tuff.

Shortly after caldera subsidence at .73 - .63 mybp rhyolite domes and flows were extruded from at least twelve eruptive centers within the caldera. Many of these centers appear to be controlled by northwest-trending faults. Contemporaneous with the eruption of these rhyolites was the formation of a resurgent dome, 10 km in diameter, in the west central portion of the caldera. The resurgent dome is transected by a 5 km-wide, complexly-faulted keystone graben that trends northwest, paralleling the major range front structures.

Following the development of the resurgent dome hornblende-biotite rhyolites were extruded in three groups, with ages of .5, .3 and .1 mybp, respectively,

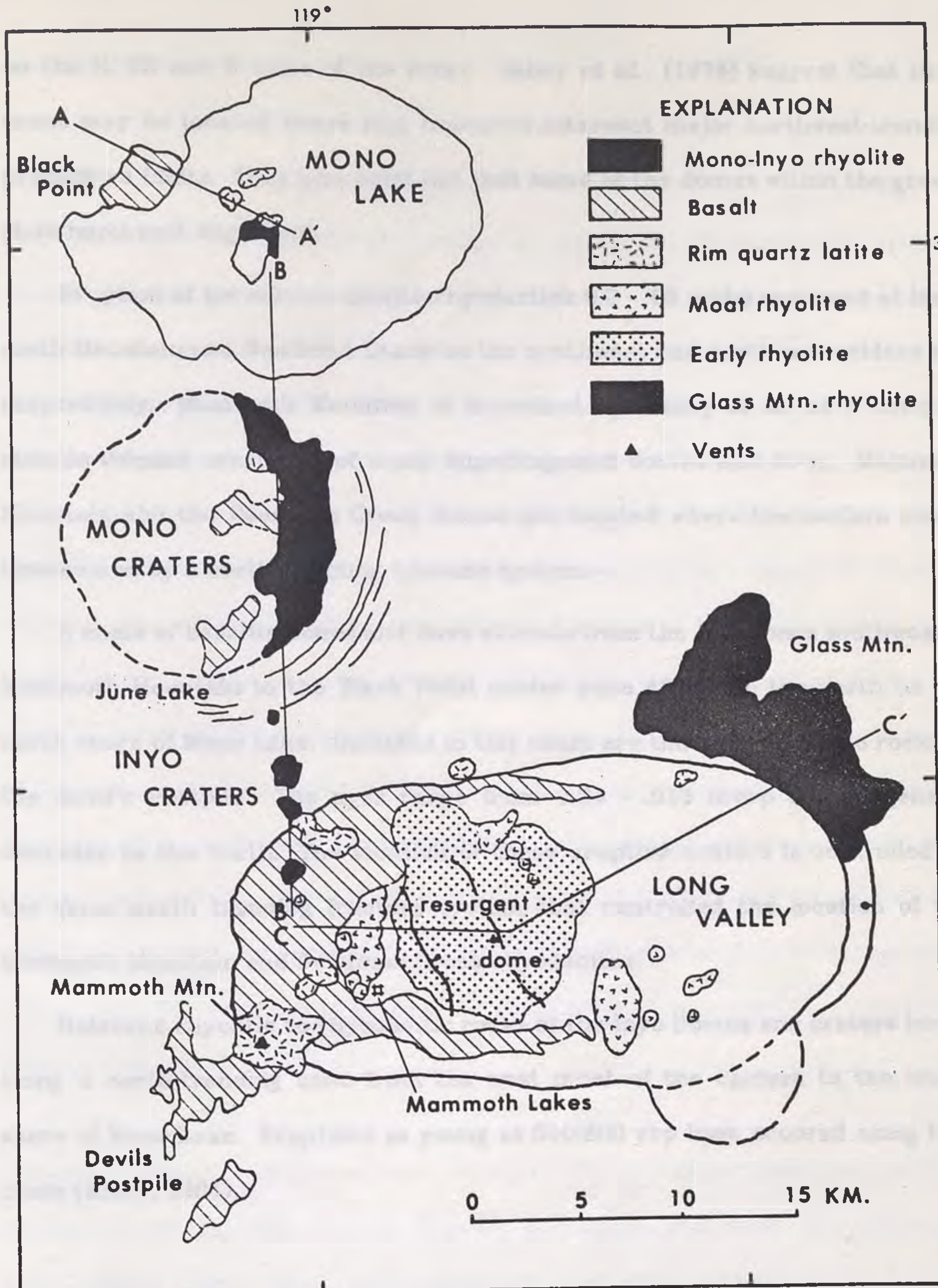

Figure 3. Geologic map showing volcanic rocks in the Long Valley area, from Bailey (1981).

on the N, SE and W sides of the dome. Bailey *et al.* (1976) suggest that these areas may be located where ring fractures intersect major northwest-trending precaldera faults. They also point out that some of the domes within the groups show northwest alignment.

Eruption of hornblende-biotite rhyodacites 0.2 - .05 mybp occurred at Mammoth Mountain and Deadman Creek on the southwest and northwest caldera rim respectively. Mammoth Mountain is described by Bailey *et al.* as a complex cumulo-volcano consisting of many superimposed domes and flows. Mammoth Mountain and the Deadman Creek domes are located where the caldera rim is intersected by a north-trending fracture system.

A chain of basaltic cones and flows extends from the Red Cones southwest of Mammoth Mountain to the Black Point cinder cone 45 km to the north on the north shore of Mono Lake. Included in this chain are the trachybasaltic rocks of the Devil's Postpile. The ages range from 0.94 - .013 mybp and in general decrease to the north. The location of these eruptive centers is controlled by the same north trending fracture system that controlled the location of the Mammoth Mountain and Deadman Creek rhyodacites.

Holocene rhyolitic to rhyodacitic rocks of the Inyo Domes and craters occur along a north-trending zone from the west moat of the caldera to the north shore of Mono Lake. Eruptions as young as 500-600 ybp have occured along this chain (Miller, 1984).

Geologic Structure

Pre-Cenozoic. The metamorphic rocks of the Mount Morrison roof pendant record several periods of regional deformation. The Paleozoic sequence is divided into three blocks by two major faults, the Laurel-Convict fault and the McGee Mountain fault (Rinehart and Ross, 1964). The Laurel-Convict fault extends from Mt. Baldwin to the mouth of Laurel Creek (refer to Figure 4). Most of the displacement on the fault predates the intrusive rocks and drag folding suggests left lateral movement (Rinehart and Ross, 1964). The McGee fault is exposed on the southwest slope of McGee Mountain. The fault is projected several miles northwest to the east side of Convict Lake and southeast to Esha Canyon on the basis of structural relationships. Numerous other pre-Cenozoic faults occur mostly in the eastern two blocks of the roof pendant. These faults trend north to northwest, have steep dips, and commonly show apparent left-lateral displacement. Several of the faults predate the granitic intrusives. The majority, however, do not bear indications of their age relative to the granitic rocks, and the sense and amount of displacement can not be determined (Rinehart and Ross, 1964).

Cenozoic. Cenozoic deformation in northern Owens Valley involves a complex pattern of faulting with warping possibly playing an important role (Bateman and Merriam, 1954). Mayo (1941) recognized four important structural trends: 1) a northwest trend roughly parallel to the San Andreas fault; 2) a northeast "cross trend" roughly parallel to the Garlock fault; 3) north-south to N30E trends; and 4) a west-northwest trend. The north-northeast structures have

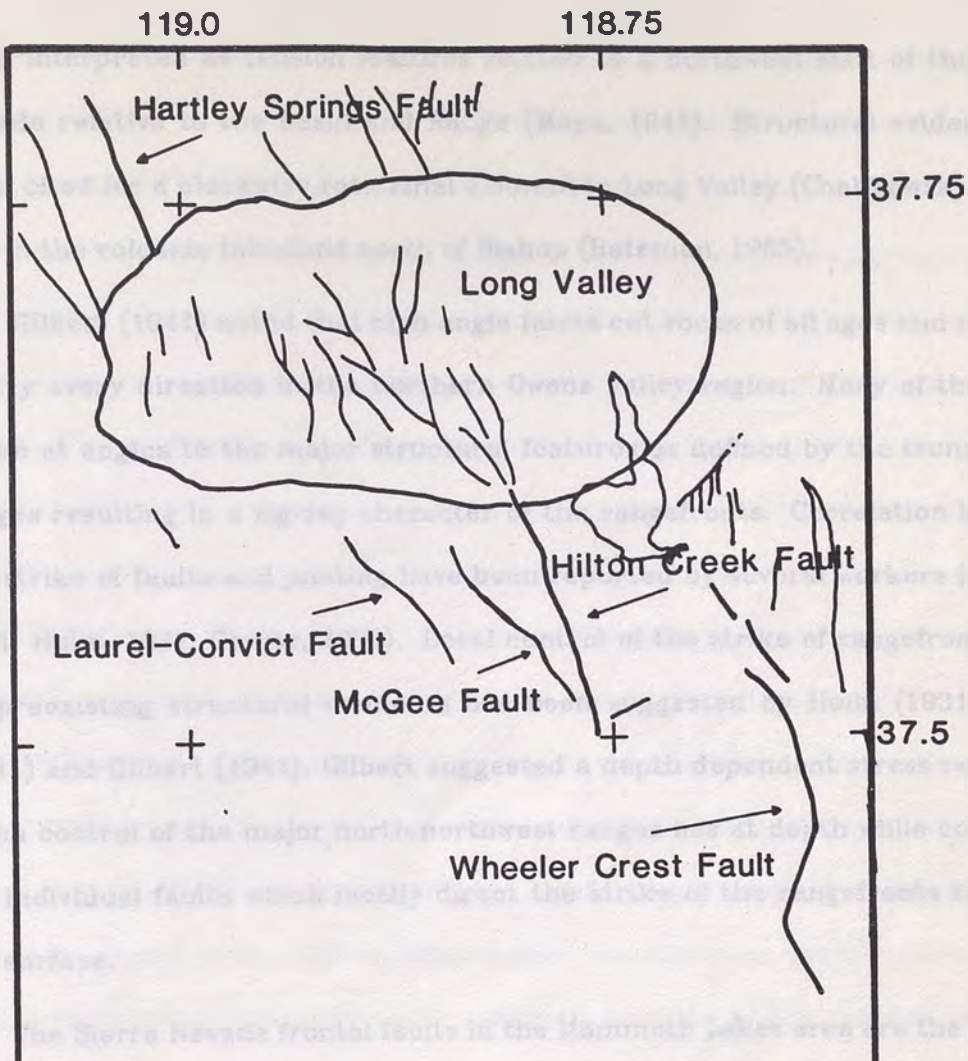

Figure 4. Map showing faults in the Mammoth Lakes/Long valley area, modified from Sorey *et al.* (1978) and Rinehart and Ross (1957).

been interpreted as tension features related to a northwest shift of the Sierra Nevada relative to the Basin and Range (Mayo, 1941). Structural evidence has been cited for a clockwise rotational element in Long Valley (Chelikowsky, 1940), and in the volcanic tableland north of Bishop (Bateman, 1965).

Gilbert (1941) noted that high angle faults cut rocks of all ages and strike in nearly every direction in the northern Owens Valley region. Many of the faults strike at angles to the major structural features as defined by the trend of the ranges resulting in a zig-zag character of the rangefronts. Correlation between the strike of faults and jointing have been reported by several workers (Gilbert, 1941; Hulin, 1931; Carver, 1970). Local control of the strike of rangefront faults by preexisting structural elements has been suggested by Hulin (1931), Mayo (1941) and Gilbert (1941). Gilbert suggested a depth dependent stress regime in which control of the major north-northwest ranges lies at depth while control of the individual faults which locally direct the strike of the rangefronts lies near the surface.

The Sierra Nevada frontal faults in the Mammoth Lakes area are the Hartley Springs, Hilton Creek and Wheeler Crest faults. These faults are shown in Figure 4. The Hartley Springs fault strikes about N15W and is mapped northwest of the caldera. Topographic relief on the fault scarp is 600 m with Tertiary andesites being displaced by 450 m and the Bishop tuff by 300 m (Bailey *et al.*, 1976). Within the caldera a zone of minor en-echelon faulting projects on strike with the fault. The "Earthquake Fault" (Benioff and Gutenburg, 1939), a local tourist attraction, is located at the southern end of this zone.

The Hilton Creek fault strikes N20W and is located at the northeast base of McGee Mountain southeast of the caldera. The Hilton Creek fault displaces lateral moraines of Tioga age (0.015-0.02 mybp) by as much as 25 m (Clark and

Gillespie, 1981) at the mouth of McGee Creek. Displacement on the fault dies out rapidly to the south and to the north; at the caldera boundary it splinters into several diverging faults.

The southern boundary of the caldera between the Hartley Springs fault and the Hilton Creek fault is a mountain front 4000 feet high. The south and southwest sections of the caldera boundary show evidence of post caldera movement. The northeast face of Mammoth Mountain is cut by a fault paralleling the caldera boundary, and older morainal ridges, thought to be of Mono Basin age, are truncated by an apparent east-west fault (Bailey *et al.*, 1976). Rinehart and Ross (1964) map EW and NW-SE faults along the caldera boundary just east of the Hilton Creek Fault. Putnam (1962) states that two dominant fault sets occur at McGee Mountain. These are N20W (Hilton Creek Fault) and N50W. His geologic map shows several faults striking N50W accross the north slope of McGee Mountain, one of which he shows cutting glacial deposits of the Convict Creek moraine. Bailey *et al.* (1976) suggest that movement on the frontal faults was accommodated on the south and southwest sections of the caldera boundary, with the recent development of faults inside the caldera indicating that it has cooled enough to allow tectonic stress to be transmitted across it. They also point out that within the caldera, the lack of "reverse drag" which is observed to the northwest and southeast of the caldera, suggests that until recently, vertical tectonic stresses were absorbed by hydrostatic adjustments within the magma chamber.

Southeast of the Hilton Creek fault the range is bounded by the Wheeler Crest fault, forming the Wheeler Crest escarpment that rises almost 6000 feet in two miles. The north face of Red Mountain, between the Hilton Creek and Wheeler Crest faults, is described as a steep ramp broken by numerous antithetic faults downthrown to the south (Rinehart and Ross, 1957). The strike of the Wheeler Crest fault varies from NNW at the north end of the fault to NNE near the south end at Pine Creek canyon. The fault dies out to the south and the rangefront steps about 10 miles (16 km) to the east across a ramplike surface (the Coyote Warp) at the north end of the Owens Valley fault zone.

East and southeast of the caldera the Bishop tuff is cut by many faults along which vertical displacement is usually less than 150 feet, with the exception of a fault intersected by the Owens Gorge Project Tunnel No. 1, which shows possibly 500 feet of displacement (Putnam, 1960). According to Putnam this fault, located just north of Long Valley Dam, is part of a major fault system striking N35E. Displacement is down to the northwest and the fault separates the Bishop tuff from lake sediments within Long Valley. He states that the faults may be responsible for the elevation of a granitic ridge, thinly veneered with Bishop tuff, that connects the Wheeler Crest on the south and the Benton Range on the north. At least a thousand feet of warping of the Bishop tuff can be demonstrated in the vicinity of Round Valley (Bateman, 1965).

In a study of steeply dipping fractures in the crystalline rocks, Mayo (1937) found that two joint trends, N30-50E and N30-50W, were favored almost everywhere in the Sierra. He found, however, that north-south fractures were abundant locally and reflect an important direction of structural weakness. He noted that west and northwest of the Rock Creek salient the N30-50W and N30-50E sets prevail, but as the salient is approached swarms of fractures striking N10-20E predominate (see figure 5).

Lockwood and Moore (1979) have interpreted much of the jointing in the Sierra as microfaulting, based on observable offsets. For most of their data set they show left-lateral motion on ENE faults and right-lateral motion on NNE

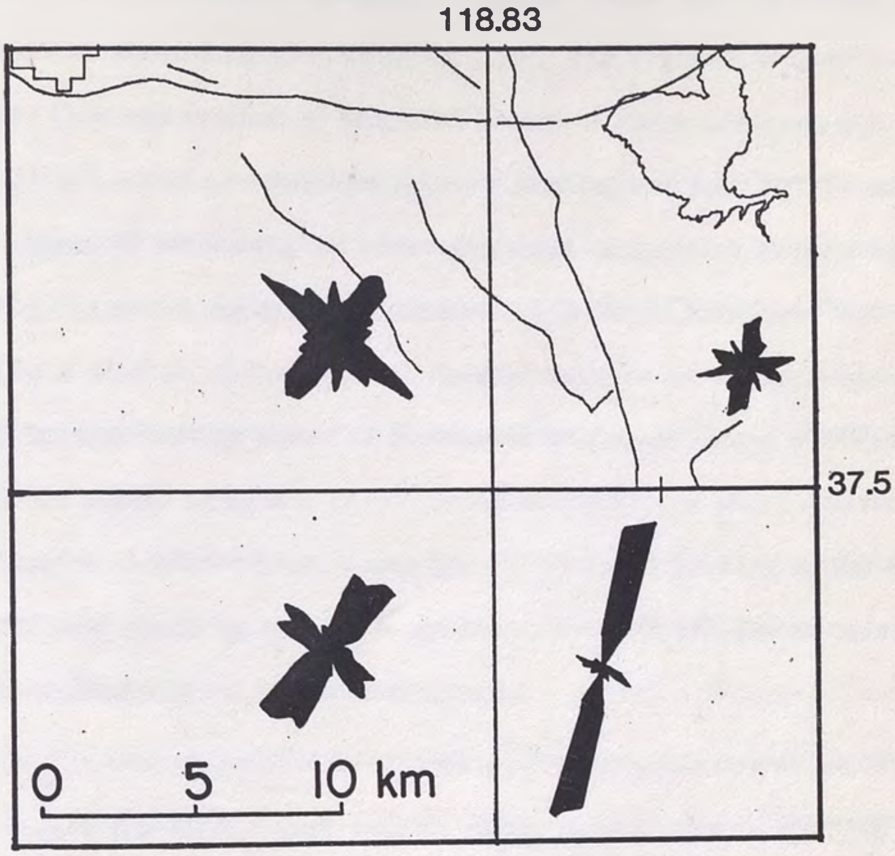

Figure 5. Map showing rose diagrams of steeply dipping joints in four areas of the Rock Creek Salient. Modified after Mayo (1937).

faults. They do, however, show evidence for NNE left-lateral microfaulting in the Mount Abbott quadrangle (south of the epicentral area).

Summary of Geologic Work

Mammoth Lakes lies in a structurally complex area positioned near the intersection of two major structural features. These are the Owens Valley rift and the Mono Basin-Excelsior Mountain Zone. The region has been the focus of extensive Cenozoic volcanism, the most recent of which occurred 500 - 600 ybp. Gilbert (1941) noted a correlation between faulting and jointing. He suggested a depth dependent stress regime where the large scale block boundaries are controlled by the stress regime at depth and the strike of individual faults are controlled by a shallow stress regime. Several authors have suggested control of faulting by pre-existing zones of structural weakness. Mayo (1937) found the Rock Creek salient to be one of four areas in the Sierra where N10-20E jointing predominates. Lockwood and Moore (1979) interpret jointing in the Sierras as conjugate microfaulting and show evidence for NNE left-lateral microfaulting near the southern end of the epicentral area.

While the overall trend of the Sierra is NNW the geometry of the range front, which defines the Rock Creek salient, shows strong control by NNE and WNW structures. Contacts between plutonic rocks within the Rock Creek salient locally exhibit NNE, NNW, and WNW trends, and cataclastic zones along contacts suggest emplacement of some of the plutons in a brittle or semi-brittle state. The similarity of the geometry of contacts between plutons within the Rock Creek salient to the trends of the range fronts that bound it suggest a relationship between the structures accomodating late Cenozoic rangefront faulting and the structures that controlled the boundaries of the Cretaceous plutons.

Chapter 2.

Seismological Investigations

Previous Work

The large earthquakes at Mammoth Lakes in May 1980 were preceded by anomalous temporal variations in the southern part of the Sierra Nevada Great Basin Boundary Zone (SNGBZ), which followed a pattern that several authors have identified as precursory to strong earthquakes (Ryall and Ryall, 1981a). The activity preceding the 1980 sequence consisted of a general decrease in seismicity in the southern SNGBZ between January 1977 and September 1978, followed by a burst of moderate earthquakes over the entire zone. The 4 October 1978 ML-5.7 Bishop earthquake was followed by earthquake swarms in the Mammoth Lakes area which migrated northwesterly with time. Figure 6, taken from Ryall and Ryall (1980), shows the northwesterly migration of activity involving NNE trending epicenters. Intense swarming occurred approximately ten days prior to the ML 6 events of 25 May 1980. Based on locations of ML 4.0 events, Cramer and Toppozada (1980) interpret the activity between September 1979 and May 1980 as involving right-lateral strike-slip faults along the southern caldera boundary. Locations of Ryall and Ryall (1981a), however, show distinct NNE trends of epicenters along the southern caldera boundary which is in agreement with the NNE-trending nodal planes of strike-slip focal mechanisms computed by Cramer and Topozada (1980) and Ryall and Ryall (1981a).

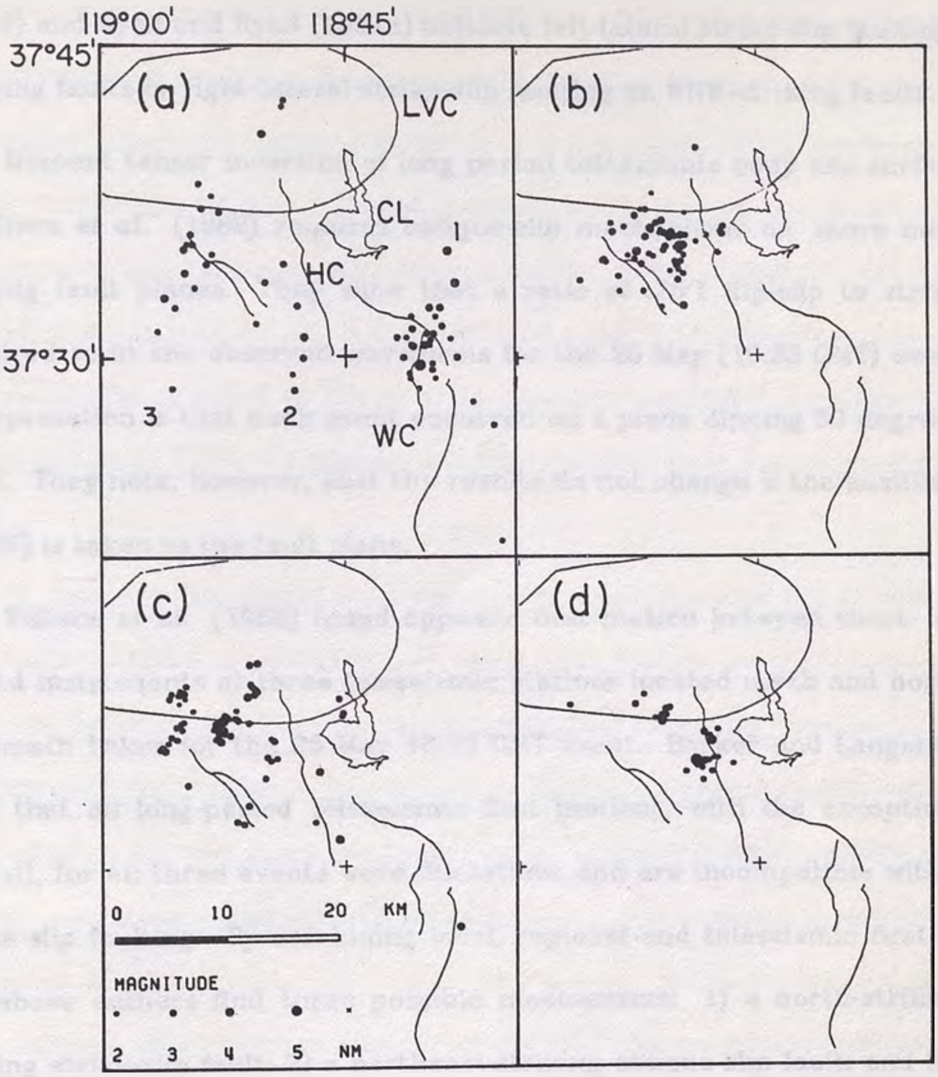

Figure 6. Map showing activity occuring during six time intervals preceeding the 1980 ML 6 events from Ryall and Ryall (1980). (a) -- 9/1/1978-11/16/1979; groups indicated by numbers are 1 -- 10/4-12/13/1978; 2 -- 2/7-3/26/1979; 3 -- 4/10-11/6/1979; (b) -- 11/7-12/18/1979; (c) -- 11/19/1979-4/17/1980; (d) -- 4/18-5/25/1980.

Source Mechanisms

Considerable controversy has arisen regarding the source mechanisms of the ML 6 events. Focal mechanisms determined by Cramer and Toppozada (1980) and Ryall and Ryall (1981a) indicate left-lateral strike-slip faulting on NNE striking faults or right-lateral strike-slip faulting on WNW-striking faults.

Moment tensor inversion of long period teleseismic body and surface waves by Given *et al.* (1982) requires oblique-slip mechanisms on more moderately dipping fault planes. They show that a ratio of .75:1 dip-slip to strike-slip is required to fit the observed waveforms for the 25 May (16:33 GMT) event. Their interpretation is that each event occurred on a plane dipping 50 degrees to the S70E. They note, however, that the results do not change if the auxilliary plane (N50W) is taken as the fault plane.

Wallace *et al.* (1982) found opposite first motion between short- and long-period instruments at three teleseismic stations located north and northeast of Mammoth Lakes for the 25 May 16:33 GMT event. Barker and Langston (1983) note that all long-period teleseismic first motions, with the exception of two (nodal), for all three events were dilatations and are incompatible with vertical strike-slip faulting. By combining local, regional and teleseismic first motions, the above authors find three possible mechanisms: 1) a north-striking, east-dipping strike-slip fault; 2) a northeast-striking oblique slip fault; and 3) a NNW-striking normal fault.

Moment-tensor inversion of long-period body and surface waves has been interpreted in terms of mechanisms with large non-double couple components (Barker and Langston, 1984; Julian, 1983; Sipkin and Julian, 1983; Ekstrom and Dziewonski, 1983; Ekstrom,1983; Wallace *et al*, 1983; Aki, 1984). Julian (1983) suggested that the 16:33 GMT and 14:50 GMT events were probably caused by fluid injection along nearly vertical fractures striking N25W to N35W. He showed that short-period first motions at all distances agree with those predicted for a compensated linear-vector dipole (CLVD) equivalent force system (Knopoff and Randall, 1970). The CLVD mechanism consists of three orthogonal force-dipoles with moments in the ratio of 2:-1:-1 with the positive force-dipole in the direction of tensile failure (ie perpendicular to the fracture). This mechanism would occur if injection of fluid occured symmetrically around the vector normal to the fracture with no net volume change (Julian, 1983). Figure 7 shows the short period first motions for the 16:33 GMT and 14:50 GMT events together with the double couple solution of Given *et al.* (1982), the nodal surfaces of Julian's (1983) proposed CLVD mechanism and nodal planes from Cramer and Toppozada (1980).

Barker and Langston (1983) found that if the moment-tensor solutions for the 16:33 GMT and 19:44 GMT events of 25 May 1980 are decomposed in terms of two orthogonal double couples the minor double couple is close to the trend of the Sierran frontal faults. They note that the major double couple will dominate the radiation pattern at all locations except near nodal planes, where the minor double couple may dominate. Therefore stations at regional to teleseismic distances south of the epicenters fall near nodes of the major double couple but near maxima of the minor double couple and will be dilatational rather than nodal.

Wallace (1983) found that for a single point source the double couple plus a CLVD as opposed to a simple double couple did not dramatically improve the fit of the synthetic to the observed waveform. He was, however, able to reduce the standard deviation by up to 40%, by paramaterizing the faulting process as a series of point sources with a change from near vertical strike-slip for the

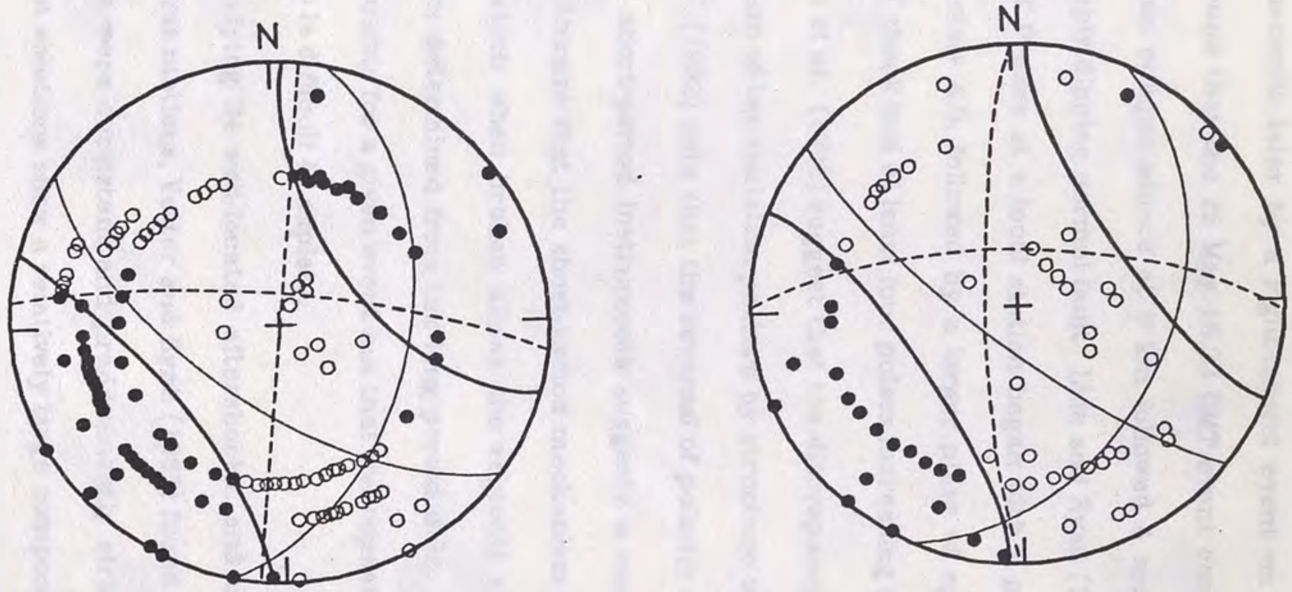

MAY 25, 1980   16 33 44.8

MAY 27, 1980   14 50 57.2

Figure 7. Lower hemisphere equal area projection showing short-period first-motions for the 25 May 16:33 GMT and 27 May 14:50 GMT events, after Julian (1983). Heavy lines -- CLVD nodal surfaces of Julian (1983); Light lines -- Moment-tensor solutions of Given *et al.* (1982); Dashed lines -- Short-period solution of Cramer and Toppozada (1980).

shallow sources to normal faulting at depth. Ekstrom (1983) states that the 16:33 GMT event is well modelled by rupture on a north-south normal fault followed 8 seconds later by a right-lateral event on an east-west fault. Wallace (1984), found that the 25 May 16:33 GMT event can be modelled with two point sources, an oblique source at 9 km followed 4 seconds later by rupture on a N20W steeply dipping normal fault. Lide and Ryall (1984) showed that the 25 May 16:33 GMT P-wave at a local station began with a pulse corresponding to ML of approximately 4.5, followed by a larger pulse of opposite polarity; the 27 May 14:50 GMT shock had at least four pulses increasing in amplitude with time.

Given *et al.* (1982) suggest that the discrepancy in mechanisms may be due to distortion of the radiation pattern by structure or to source complexity. Wallace *et al.* (1982) note that the reversal of polarity at the same station between long- and short-period instruments suggests a complex source-time function. They hypothesize that the short-period mechanism may represent failure of an asperity which when broken allows the regional strain to be relieved by the mechanism determined from the long-period data. They note that this process seems plausible for a given event but that the repeatability of this process for all the events is difficult to explain.

In studying 34 well-located aftershocks, and using short-period local and regional first motions, Vetter and Ryall (1983) found that events with depths less than 9 km were consistent and predominantly strike-slip, whereas for greater depth most solutions show a relatively large component of normal slip and some show almost pure normal faulting. They found that there were some strike-slip events at depths greater than 9 km but almost no shallow events with a predominant normal component. Figure 8 shows the focal mechanisms determined for events shallower than 9 km and Figure 9 shows the focal mechanisms for events

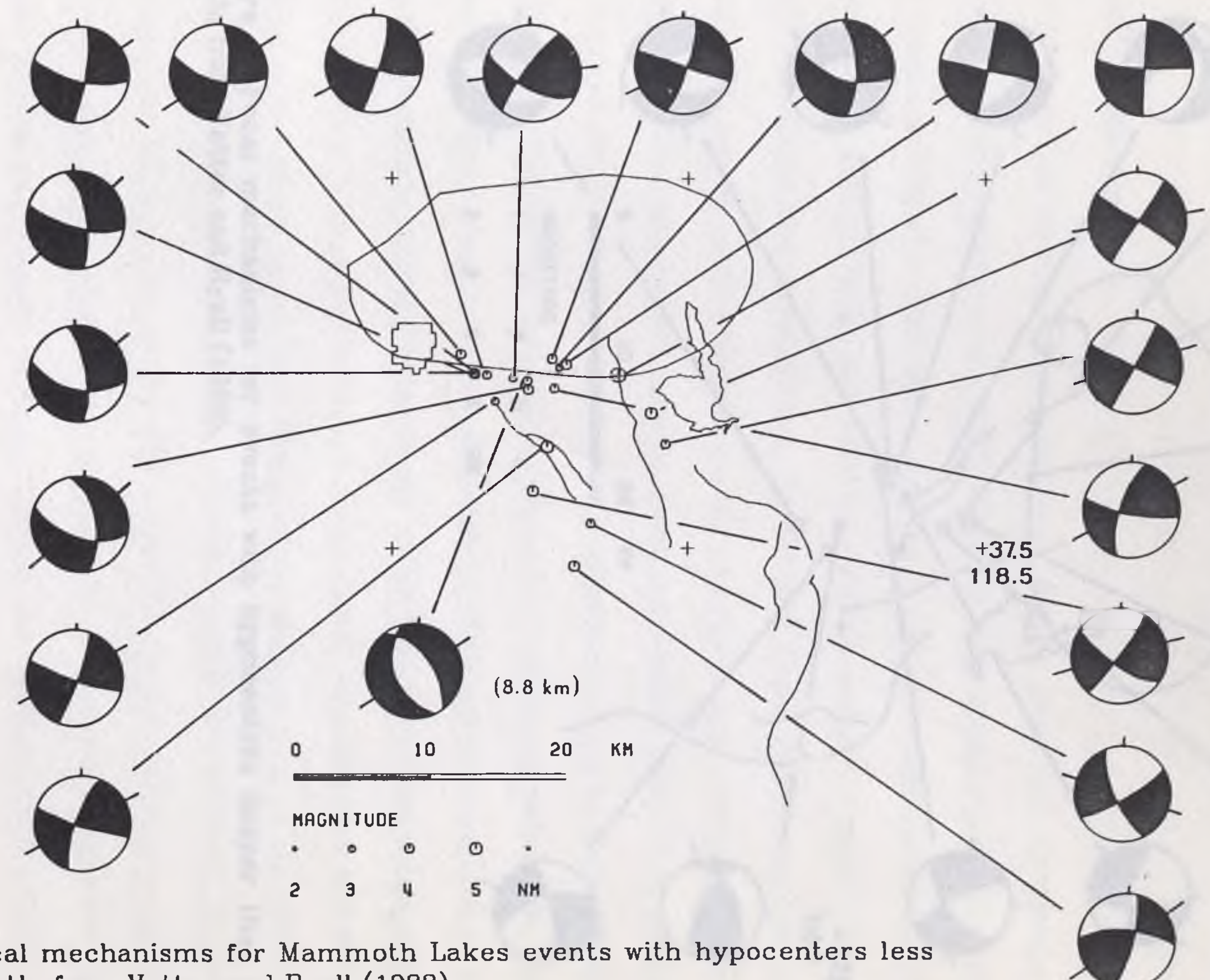

Figure 8. Focal mechanisms for Mammoth Lakes events with hypocenters less than 9 km depth, from Vetter and Ryall (1983).

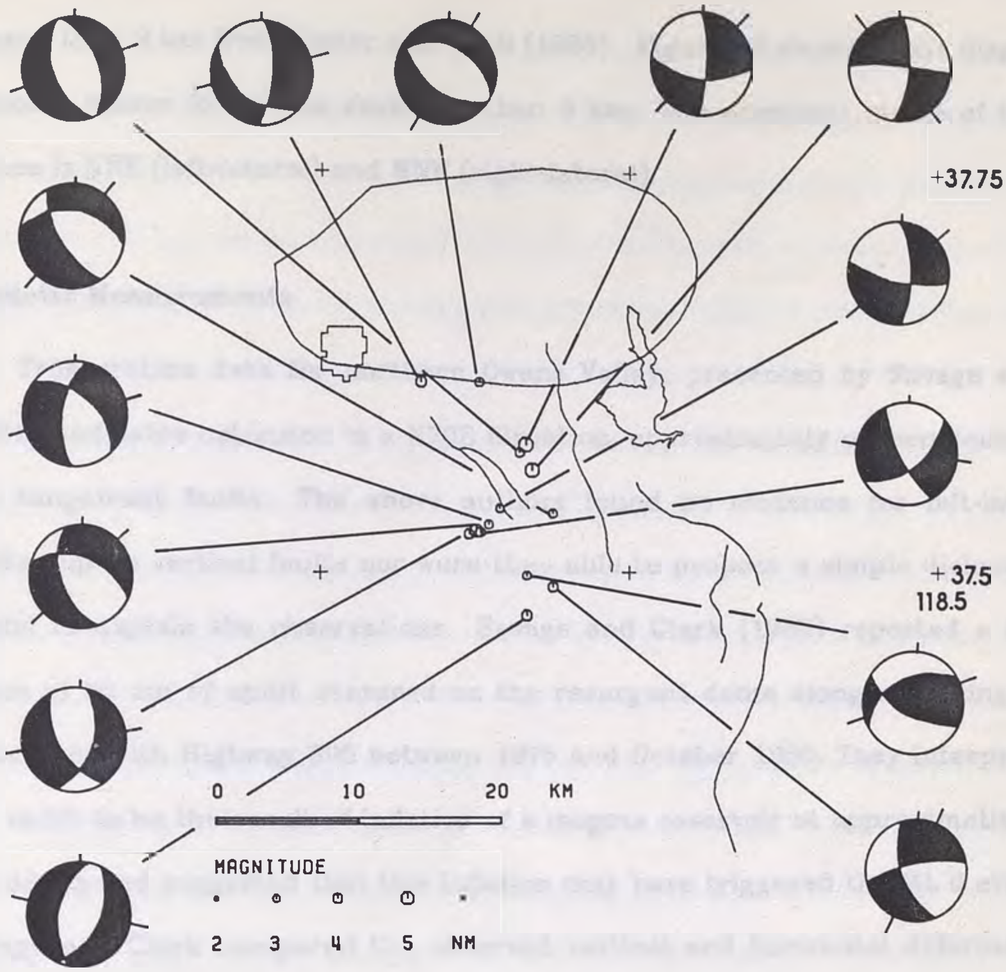

Figure 9. Focal mechanisms for events with hypocenters deeper than 9 km depth, from Vetter and Ryall (1983).

deeper than 9 km from Vetter and Ryall (1983). Figure 19 shows a rose diagram of nodal planes for events shallower than 9 km. The dominant strike of these planes is NNE (left-lateral) and WNW (right-lateral).

Geodetic Measurements

Trilateration data for northern Owens Valley, presented by Savage *et al.* (1981), indicates extension in a N70E direction, approximately perpendicular to the rangefront faults. The above authors found no evidence for left-lateral strike slip on vertical faults nor were they able to propose a simple dislocation model to explain the observations. Savage and Clark (1982) reported a maximum of 25 cm of uplift centered on the resurgent dome along a leveling line coincident with Highway 395 between 1975 and October 1980. They interpreted the uplift to be the result of inflation of a magma reservoir at approximatley 10 km depth and suggested that this inflation may have triggered the ML 6 events. Savage and Clark compared the observed vertical and horizontal deformation with that calculated for the inflation, by .15 km^3, of a spherical magma chamber with its center 11 km beneath the resurgent dome. The observed and calculated vertical deformation agreed well except where the line crossed the Hilton Creek fault, which they explained by the observed normal displacement on the fault following the ML 6 events of May 1980. The horizontal deformation agrees less well but a reasonably good fit was obtained at all stations except for those at Laurel Canyon and Sherwin Summit. Savage and Clark attributed this to coseismic deformation, as these were the two closest stations to the ML 6 events. They also noted that the northerly displacement observed at both stations could not be explained by left-lateral strike-slip on a north striking vertical plane in the vicinity of the ML 6 events. However, they pointed out that the proposed magma injection would increase left-lateral shear stress on north trending planes in the vicinity of the 16:33, 19:44, and 14:50 GMT events as well as the 1978 Bishop event. It should be noted that the best agreement between the observed and calculated horizontal displacements occurs at stations where the displacement calculated for the magma injection model is close to the same direction as that of regional extension.

Rundle and Whitcomb (1984) state that faulting and seismicity appear to be driven by magma injection and proposed a model involving the sequential inflation of two magma chambers. The locations of these chambers is consistant with zones of S-wave shadowing reported by Ryall and Ryall (1981b), Sanders and Ryall (1983), and Sanders (1984). The model consists of a magma chamber at 9 km depth in the northeast portion of the caldera, the inflation of which caused the observed uplift in 1980, and a second magma chamber at 5 km depth near Casa Diablo Hot Springs. Rundle and Whitcomb propose that inflation of these magma chambers was the driving mechanism for right-lateral and normal faulting beneath the south moat and left-lateral and normal faulting on the Hilton Creek fault.

Deformation associated with an intense swarm along the southern caldera boundary was interpreted by Savage and Cockerham (1984) as resulting from a combination of dike intrusion and right-lateral faulting on a north dipping listric surface striking WNW beneath the south moat.

Spasmodic Tremor

Following the ML 6 events of May 1980, intensive swarms of earthquakes began to occur in a small area on the southwest boundary of the caldera.(see Fig. 13). These swarms typically lasted for 1-2 hours, produced hundreds of microearthquakes and had the appearance of spasmodic tremor observed in volcanic regions (Ryall and Ryall,1981b). The first swarm of this type occured on 3 July 1980 and to date nine periods of activity of this type have been observed. These distinct bursts of activity are interpreted by Ryall and Ryall as marking an area of intense fracturing, due to magma injection or gas expelled under high pressure from a magma body.

Attenuation of S-waves

Ryall and Ryall (1981b) observed drastic attenuation of S-wave amplitudes and the absence of frequencies higher than about 2-3 HZ in P-waves for raypaths passing through certain portions of the caldera. The S-wave shadowing suggests that the raypaths passed through bodies of magma. They found that a region in the south-central caldera was responsible for the S-wave attenuation. More detailed work by Sanders and Ryall (1984) defined a large magma body in the south central portion of the caldera extending from 4.5 km to at least 13 km in depth. A second body of magma was located in the northwest portion of the caldera. Sanders (1984) analyzed 1200 raypaths through the caldera and mapped the geometry of two massive magma bodies in the central and northwestern parts of the caldera. The central body is less well defined but lies beneath the keystone graben of the resurgent dome and is as shallow as 4.5 km. The northwestern magma body lies between 5.5 km and at least 13 km in depth. He also located two areas, one just south of the central magma body and the other beneath Lake Crowley, which he interprets as areas containing dikes, pipes and/or sills. Ryall and Ryall (1984) report that anomalous attenuation is also observed for earthquakes and stations in the area south of Long Valley caldera, and conclude that a zone of magma extends at least 10-12 km south of the caldera. Ryall and Ryall (1984) report that anomalous attenuation is also observed for earthquakes and stations in the area south of Long Valley caldera, and conclude that a zone of magma extends at least 10-12 km south of the caldera.

Crustal Structure

Evidence for a thick crust or root beneath the Sierra Nevada was first presented by Byerly (1938). Eaton (1966) analyzed a reversed refraction line between Shasta Lake and China Lake and presented evidence for a three-layered crust 54 km thick beneath the high southern Sierras.

Prodehl (1979), concluded that the velocity does not exceed 6.1 km/sec in the upper 20 km of the crust for a profile from China Lake to Mono Lake. He found that the average P-wave velocity between 20 km and approximately 35 km to be 6.4 - 6.6 km/sec in the vicinity of Mono Lake. Below 35 km the velocity begins to increase to 7.6-7.8 km/sec at the base of the crust.

Refraction profiles within Long Valley (Hill, 1976) suggest that the basement (Vp = 6.0±.4 km/sec) lies between 3 and 4 km depth in the north and east parts of the caldera and between 1.5 and 2 km in the west central and southwestern portions. A 1-2 km thick unit with velocity 4.0-4.4 km/sec forms a continuous layer above the basement. Material with velocities of 2.7-3.4 km/sec lies between that unit and a 1.5-1.9 km/sec surficial layer. Thickness of the surficial layer varies from 50 - 200 m in the western part of the caldera to at least 500 m thick in the eastern part of the caldera.

Chapter 3 -

Precise Locations of Aftershocks

Instrumentation

Prior to the ML 6 events of May 1980 the University of Nevada Seismological Laboratory (UNSL) operated stations CLK, LMC, ORC, BON and MON in the Mammoth Lakes/ northern Owens Valley area (refer to Fig. 10). In addition, two digital event recorders were operated at the Mammoth Ranger Station (MRS) and at Buzztail Springs in McGee Creek Canyon(MCG). Unfortunately, station MCG ran out of tape and did not record the ML 6 events on 25 May. It did, however, record the 14:50 GMT ML 6.2 event on 27 May. Following the main shocks, we deployed six portable, centrally-recording analog seismographs in the epicentral area. These stations (MLA-F in Fig. 10) began recording on 28 May and operated until 31 July 1980. Due to equipment malfunction, no data was recorded on this system for the periods June 5-12 and July 3 - 11.

The U. S. Geological Survey (USGS) deployed several three-component portable seismographs in the epicentral area. USGS stations utilized in this study were EDL and SHR.

Due to the inaccessability of the epicentral area there is a lack of station coverage to the west at close distances. The USGS portable station (EDL) at Lake Thomas Edison is in a critical location but is approximately 20 km southwest of the epicentral area. This station operated from 31 May until 13 June and, unfortunately, the UNSL portable stations were down for just over half of this period. The next closest station to the west is Friant (FRI), which is operated by the University of California Berkeley and is approximately 100 km distant.

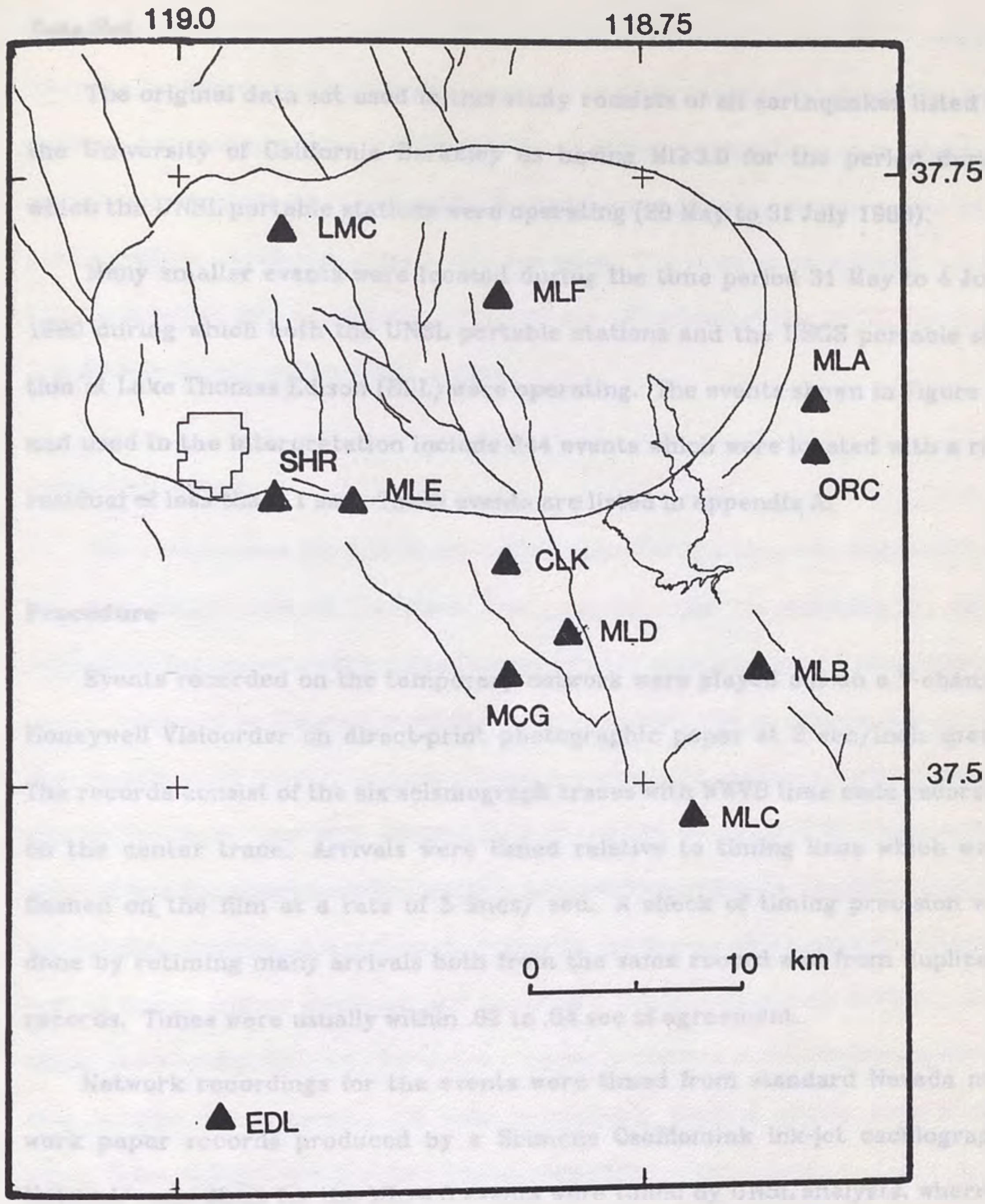

Figure 10. Locations of stations operated by UNSL and USGS in the Mammoth Lakes area following the 1980 ML 6 events which were used for this study.

Data Set

The original data set used in this study consists of all earthquakes listed by the University of California Berkeley as having Ml≧3.0 for the period during which the UNSL portable stations were operating (28 May to 31 July 1980).

Many smaller events were located during the time period 31 May to 4 June 1980 during which both the UNSL portable stations and the USGS portable station at Lake Thomas Edison (EDL) were operating. The events shown in Figure 13 and used in the interpretation include 344 events which were located with a rms residual of less than .1 sec. These events are listed in appendix A.

Procedure

Events recorded on the temporary network were played out on a 7-channel Honeywell Visicorder on direct-print photographic paper at 2 sec/inch speed. The records consist of the six seismograph traces with WWVB time code recorded on the center trace. Arrivals were timed relative to timing lines which were flashed on the film at a rate of 5 lines/ sec. A check of timing precision was done by retiming many arrivals both from the same record and from duplicate records. Times were usually within .02 to .04 sec of agreement.

Network recordings for the events were timed from standard Nevada network paper records produced by a Scimens Oscillomink ink-jet oscillograph. Network recordings for the ML>4.0 events were timed by UNSL analysts, whereas smaller events were timed by the author. Cross checking showed that picks by different analysts were usually within .02 to .05 seconds.

Readings for the station FRI were made from the original Develocorder records at the seismographic station of the University of California Berkeley to a precision of ± 0.02 sec.

Paper records from stations EDL and SHR were made at the USGS, using a Seimens Oscillomink. The records consisted of six seismograph traces (two gain settings for each component) with WWVB and internal clock time code recorded on top and bottom of the record. A square-wave signal generator was used periodically to check the alignment of the pens. The records were timed using a digitizing tablet with a resolution of 0.001 inch. Precision of the timing for sharp breaks was usually within ±0.01 second.

Location Program

The events used for this study were located with a program which utilizes Geiger's (1912) inversion method. The program uses no weighting or depth fixing and also incorporates station elevation in computing travel times. In many cases, solutions by Geiger's method become unstable due to matrix singularity. This results most often from poor station coverage and shallow events where the change in travel time with respect to a change in depth ($\partial T / \partial z$) approaches zero. Since the purpose of this study is to produce precise earthquake locations for detailed analysis, it was thought better to use events which pass the rigorous test of linear matrix inversion and to discard those events with unstable solutions. Admittedly, this may be at the expense of shallow events or events occurring outside the network, but such imprecisely located events may hinder recognition of the pattern of well-located events.

Use of station elevations in the computation has at least two advantages. For shallow events, $\partial T / \partial z$ approaches zero less rapidly for a non-planar station distribution. Secondly the computed residuals are due entirely to velocity heterogeneity and/or timing errors. This is a more accurate method than assuming a planar station geometry and applying constant corrections for elevation, since the effect of elevation varies with angle of incidence. This is particularly true when using local stations in an area of high relief such as the Mammoth Lakes area, where the difference in station elevation is as great as 650 m.

Velocity Model

Two construction blasts at Mammoth Mountain were recorded in October 1982. Locations of the blasts were such that three stations (LCC, SHL and CLK) along, but outside the southern caldera boundary fell very close to a straight line from the blast. The three stations ranged from 7-19 km in distance and first arrivals yielded a velocity of 5.8 km/sec. In August 1983 a blast at Minaret Summit was conducted by the USGS. The location of this blast was in the same azimuth with respect to a line connecting the same stations. Only stations LCC and CLK recorded this blast and they were located at 13.5 km and 21.9 km, respectively. The first arrivals at these stations defined a velocity of 5.8 km/sec with an intercept of .52 sec. Combining data from the Mammoth Mountain blasts (shown in a reduced traveltime curve in Figure 11) suggests that the 5.8 km/sec arrivals emerge at least as close as 7 km. A line through the origin to the arrival at 7 km gives a velocity of 4.0 km/sec. Assuming a two-layer structure and using the intercept time gives a thickness of 1.5 km for a 4.0 km/sec layer.

The velocity model chosen was a half-space model. Since no stations at distances greater than 100 km were used in the locations an upper-mantle layer is not needed. While data for shallow velocity structure within the mountain block is all but absent, the observations presented above suggest that a velocity of 5.8 km/sec is appropriate at 1.5 km depth and probably less. Within the mountains a layered structure, i.e., a sharp horizontal interface with a large velocity contrast is unlikely. The velocity structure is probably more similar to a gradient

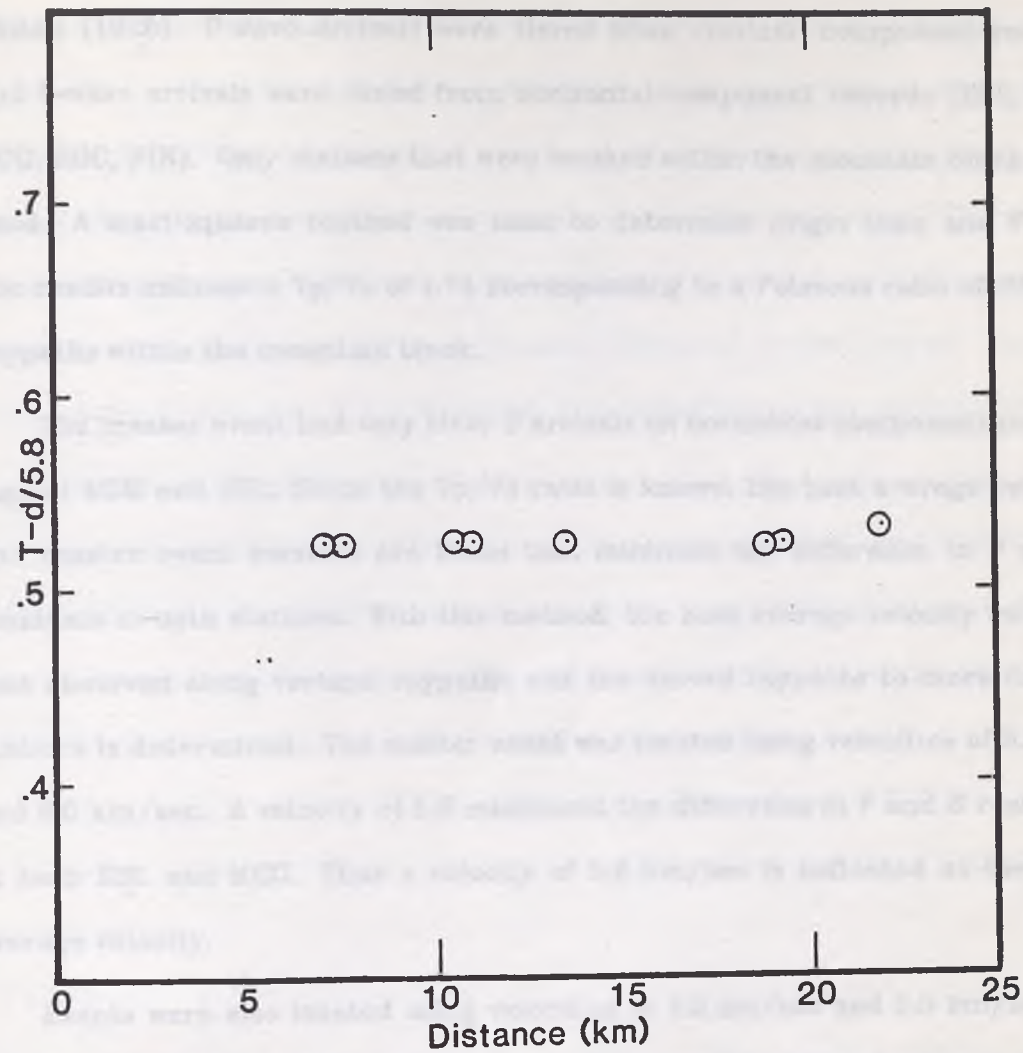

Figure 11. Reduced travel-time curve using combined data from Mammoth Mountain, Minaret Summit and Mono Pass blasts.

with a gradual increase in velocity with depth.

A study of the ratio of P to S velocities was conducted using the method of Wadati (1928). P-wave arrivals were timed from vertical- component records and S-wave arrivals were timed from horizontal-component records (EDL, SHR, MCG, ROC, PIN). Only stations that were located within the mountain block were used. A least-squares method was used to determine origin time and Vp/Vs. The results indicate a Vp/Vs of 1.74 corresponding to a Poissons ratio of .253 for raypaths within the mountain block.

The master event had very clear S arrivals on horizontal component recordings at MCG and EDL. Since the Vp/Vs ratio is known, the best average velocity and master event location are those that minimize the difference in P and S residuals at both stations. With this method, the best average velocity between that observed along vertical raypaths and the curved raypaths to more distant stations is determined. The master event was located using velocities of 5.5, 5.8 and 6.0 km/sec. A velocity of 5.8 minimized the difference in P and S residuals at both EDL and MCG. Thus a velocity of 5.8 km/sec is indicated as the best average velocity.

Events were also located using velocities of 5.5 km/sec and 6.0 km/sec. It was found that the relative locations and patterns of the aftershocks were consistent but that the whole epicentral zone was shifted. Event locations using 6.0 km/sec were shifted approximately 2 km N35E relative to locations using 5.5 km/sec.

Method

A master-event technique was employed in locating the events. Selection of the master event (31 May 08:05 GMT) was based on the following criteria: 1) the event was centrally located, both with respect to the epicentral area as well as to the first, third and fourth ML 6 events; 2) the event occurred during a time period when station distribution allowed location of the event using only stations within the mountains; and 3) the event was located close (1.2 km NW) to a digital event recorder (MCG) operating at Buzztail Springs in McGee Canyon. This station recorded very clear P and S arrivals which constrained the depth to 9.2 km.

The use of a master event that was well located using only stations within the mountains removes any bias toward the mountains that may result from using stations on low-velocity caldera fill. Travel time residuals at each station were used as corrections for locating the events relative to the master event. Table 1 lists the residuals at each station for the master event.

Table 1. Traveltime residuals from the master event location.

Sta.	P	S	Sta.	P	S	Sta.	P	S
BON	-0.50		*MCG	-0.02	0.03	*MLE	-0.02	
*CLK	0.03		MLA	-0.14		MLF	0.08	
*EDL	-0.01	0.02	*MLB	0.05		MON	-0.14	
FRI	-0.75		*MLC	-0.03		ORC	-0.11	
LMC	0.26		*MLD	-0.06		*SHR	0.01	

* stations used in locating master event

Figure 12 shows station distance and azimuth from the master event for those stations used in the location.

Results

Figure 13 shows the location of afershocks with calculated rms residuals of less than .1 second relative to the master event. The epicenters define a triangular zone located below the mountains south of the caldera. A broad WNW trending zone of epicenters occurs along the southern caldera boundary and forms the northern boundary of the activity. Most of the activity occurs between the Hilton Creek fault and an apparent linear boundary on the southwest. This boundary is on strike with the Hartley Springs fault north of Long Valley caldera and is parallel to the Hilton Creek fault.

The most obvious features of the locations are the two nearly perpendicular trends striking WNW and NNE. Two NNE trending parallel zones of epicenters are evident south of the caldera. The southeastern zone is particularly well expressed. Figure 14 shows the depth section A-A' in the N75W-S75E direction

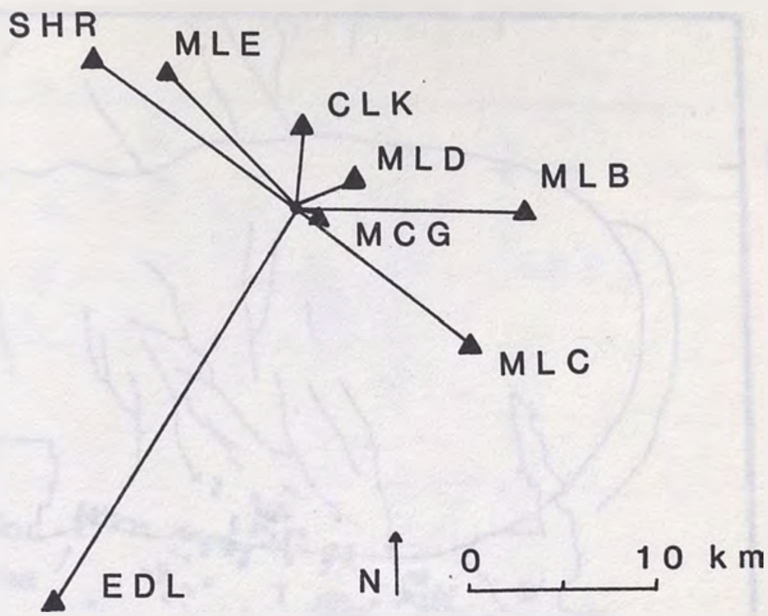

Figure 12. Distance and azimuth from the master event to stations used in the location.

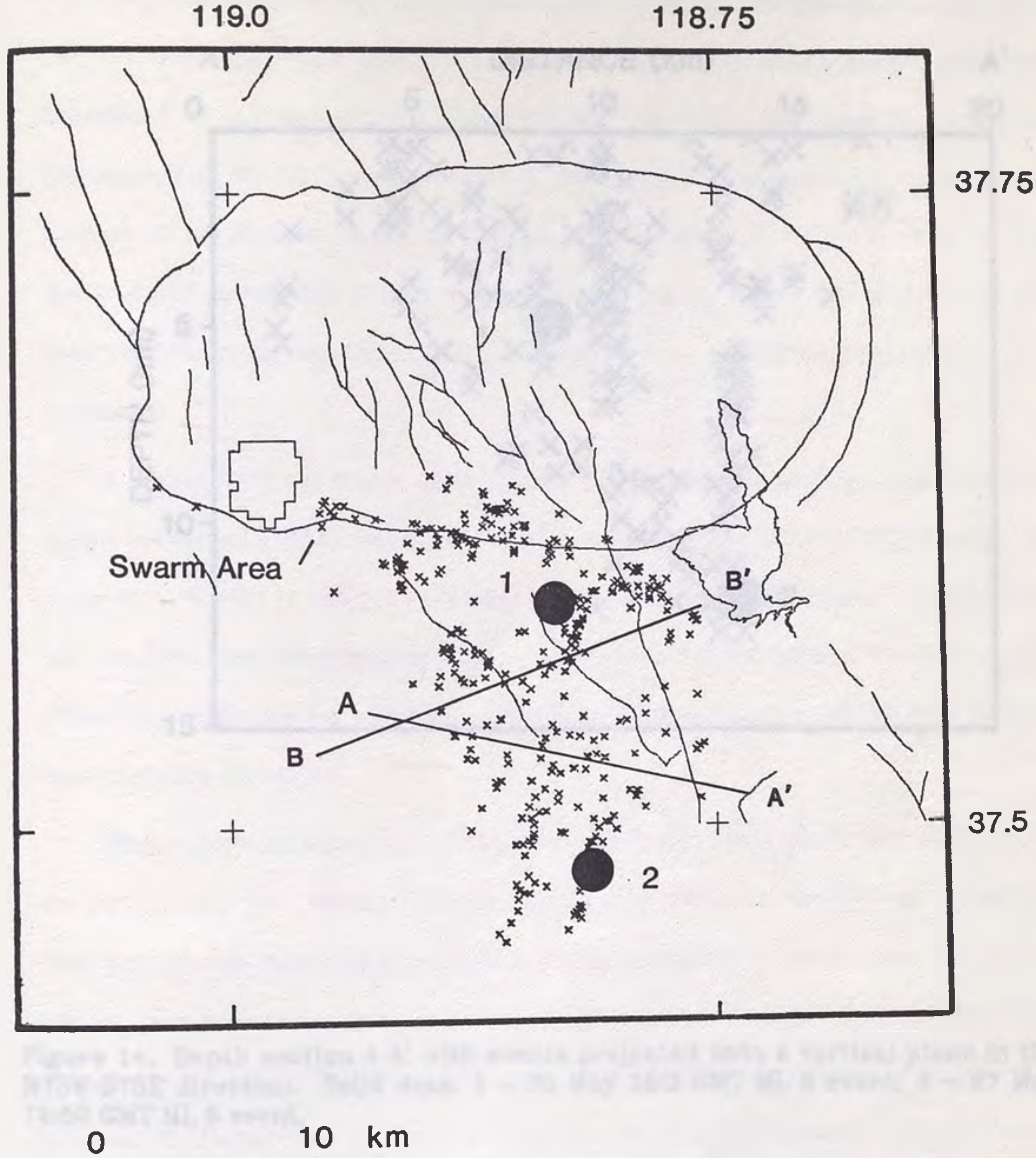

Figure 13. Epicenters of 344 aftershocks which were located with an RMS residual of .1 sec. or less. Solid dots; 1 -- 25 May 16:33 GMT ML 6 event; 2 -- 27 May 14:50 GMT ML 6 event.

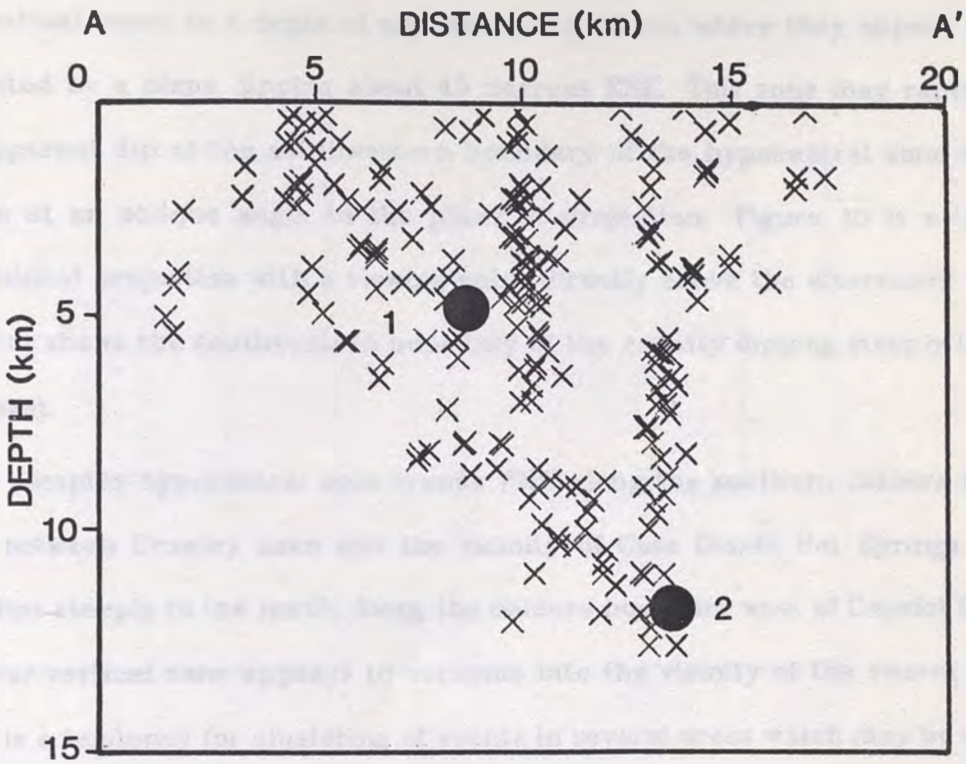

Figure 14. Depth section A-A' with events projected onto a vertical plane in the N75W-S75E direction. Solid dots: 1 -- 25 May 16:3 GMT ML 6 event; 2 -- 27 May 14:50 GMT ML 6 event.

on which the hypocenters south of the caldera boundary have been projected. Hypocenters south of the caldera boundary along the southeastern edge define two vertical zones to a depth of approximately 10 km where they appear to be truncated by a plane dipping about 45 degrees ESE. This zone may represent the apparent dip of the southwestern boundary of the hypocentral zone which strikes at an oblique angle to the plane of projection. Figure 15 is a three-dimensional projection with a viewing point directly above the aftershock zone. This plot shows the southwestern boundary of the activity dipping steeply to the northeast.

A complex hypocentral zone trends WNW along the southern caldera boundary, between Crowley Lake and the vicinity of Casa Diablo Hot Springs. This zone dips steeply to the north. Along the caldera boundary west of Convict Creek the near-vertical zone appears to continue into the vicinity of the swarm area. There is a tendency for clustering of events in several areas which may be zones where planes intersect.

The southwest boundary of the epicentral zone is a sharp linear boundary, on strike with the Hartley Springs fault and parallel to the Hilton Creek fault. This part of the zone has poor station coverage and as a result poor depth resolution, particularly for shallow events. Figure 16 shows the depth section B-B' in the direction N70E-S70W on which only events which were located south of the caldera boundary are projected. The southwestern boundary appears to dip steeply to the northeast. Figure 17 shows the locations of events with hypocentral depths of 8 km and greater. These events occur in a much narrower zone, which in general, has a trend parallel to NNW striking rangefront faults.

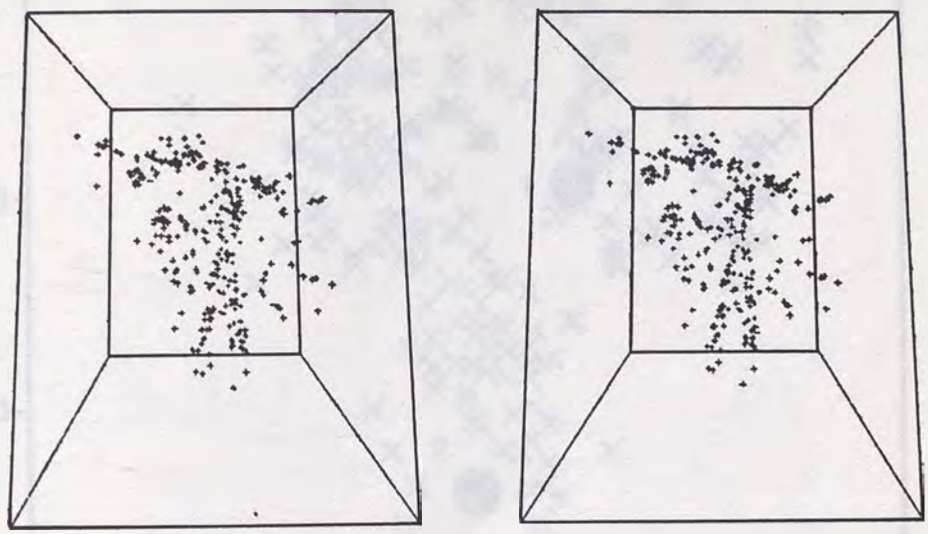

Figure 15. Three-dimensional projection of aftershocks with viewing point directly above center of epicentral zone.

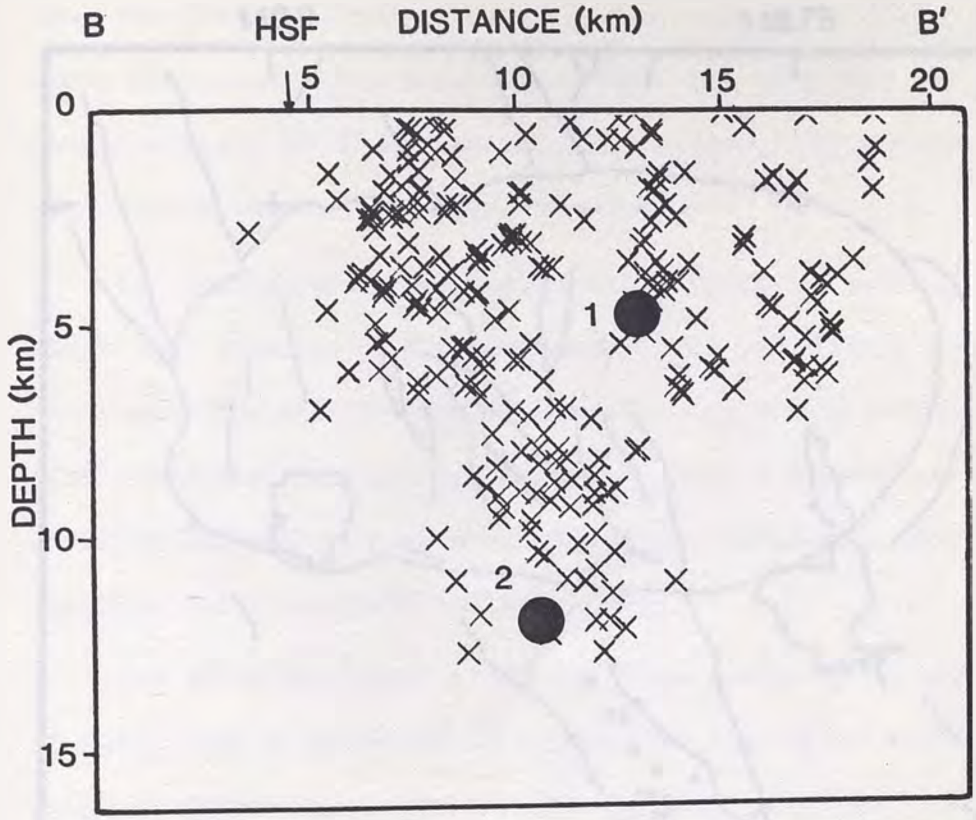

Figure 16. Depth section B-B' with events projected onto a vertical plane in the N70E-S70W direction. Solid dots: (1) -- 25 May 16:33 GMT ML 6 event; (2) -- 27 May 14:50 GMT ML 6 event. HSF -- Surface trace of the Hartley Springs fault projected onto the plane of cross-section.

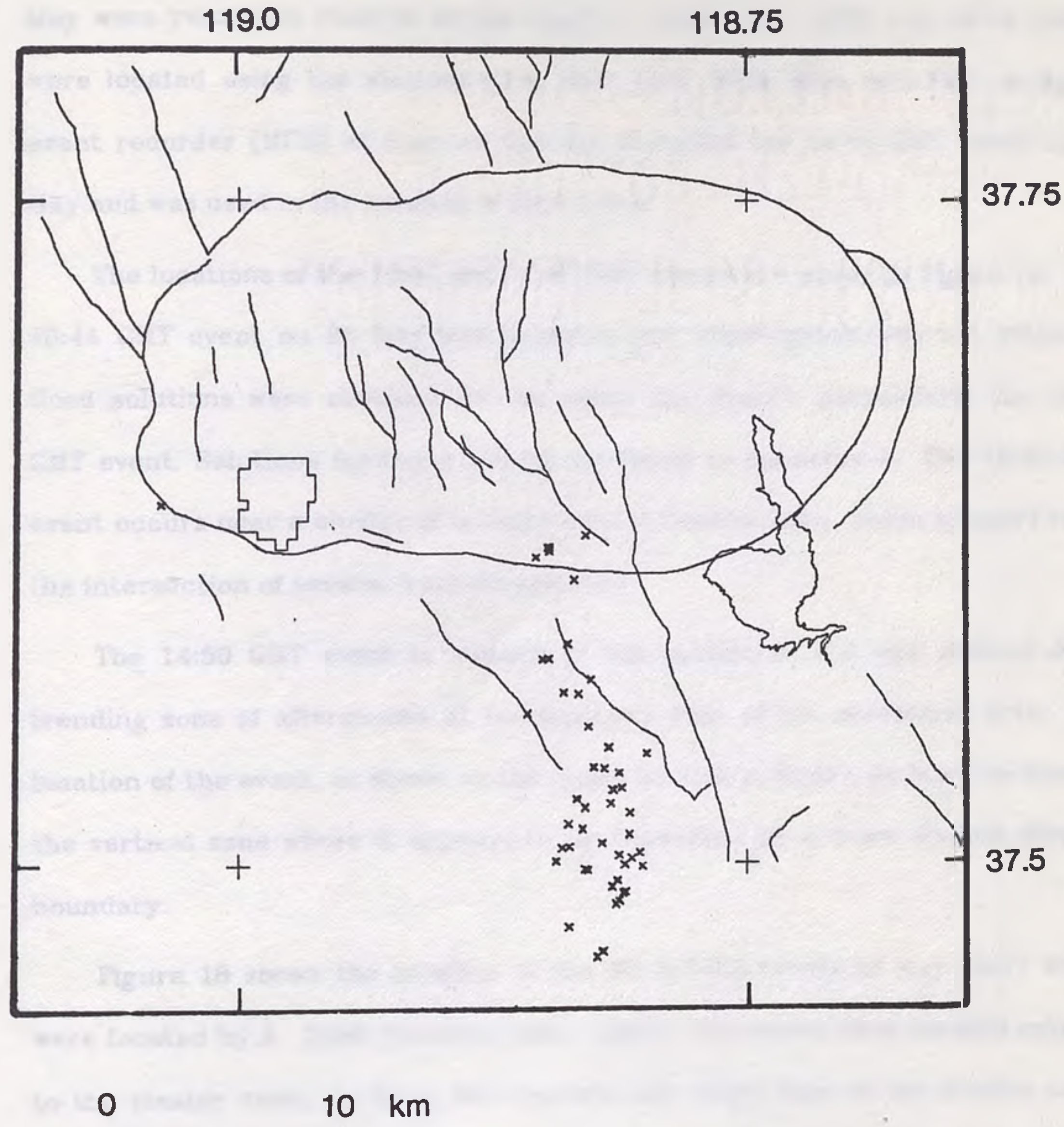

Figure 17. Epicenters of aftershocks with depths of 8 km or greater.

Location of ML 6 Events

The ML 6 events of 16:33 GMT and 19:44 GMT on 25 May and 14:50 GMT on 27 May were relocated relative to the master event. The 16:33 and 19:44 events were located using the stations CLK, LMC, ORC, MON, BON, and FRI. A digital event recorder (MCG) at Buzztail Springs recorded the 14:50 GMT event on 27 May and was used in the location of that event.

The locations of the 16:33 and 14:50 GMT events are shown in Figure 13. The 19:44 GMT event on 25 May was unstable and convergence was not attained. Good solutions were obtained for the other two events, particularly the 14:50 GMT event. Solutions for these events are listed in Appendix A. The 16:33 GMT event occurs near a cluster of activity east of Convict Lake, which appears to be the intersection of several fracture systems.

The 14:50 GMT event is located in the middle of the well defined NNE-trending zone of aftershocks at the southern edge of the epicentral area. The location of the event, as shown on the depth section in Figure 14 is at the base of the vertical zone where it appears to be truncated by a more shallow dipping boundary.

Figure 18 shows the location of the ML 5.7-6.3 events of May 25-27 which were located by A. Ryall (personal com. 1984). The events were located relative to the master event by fixing the location and origin time of the master event and computing corrections to all stations. The locations of the 25 May 16:33 GMT and the 27 May 14:50 GMT events are in relatively good agreement with those obtained using the simple location routine.

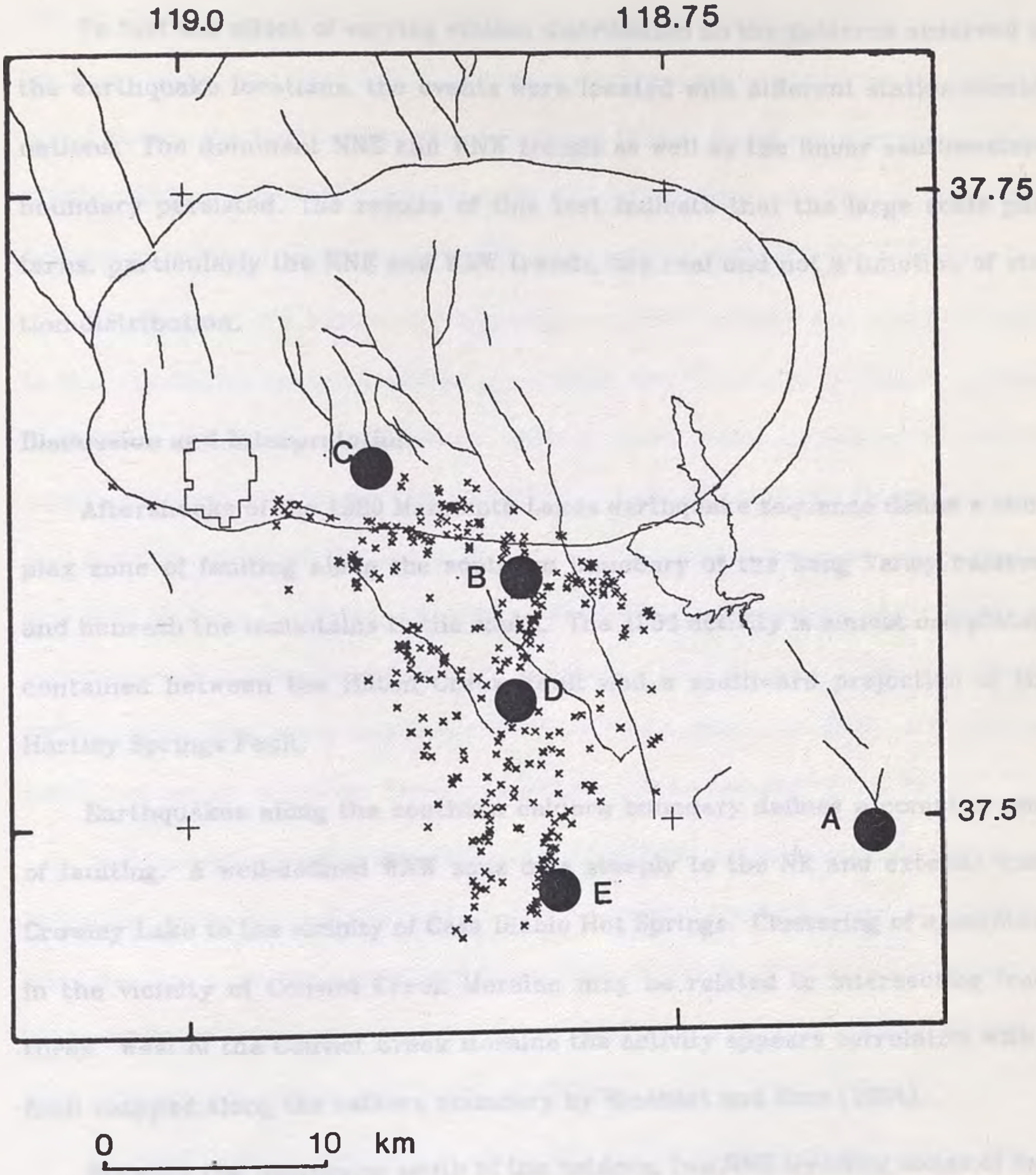

Figure 18. Epicenters of the four ML 6 events of May 1980 and the ML 5.7 event of October 1978 (solid dots) which were located using HYPO71r (Lee and Lahr, 1975) shown with aftershocks. A -- 4 Oct. 1978; B -- 16:33 GMT 25 May; C -- 16:49 GMT 25 May; D -- 19:44 GMT 25 May; E -- 14:50 GMT 27 May.

Effects of Station Distribution

To test the effect of varying station distribution on the patterns observed in the earthquake locations, the events were located with different station combinations. The dominant NNE and WNW trends as well as the linear southwestern boundary persisted. The results of this test indicate that the large scale patterns, particularly the NNE and WNW trends, are real and not a function of station distribution.

Discussion and Interpretation

Aftershocks of the 1980 Mammoth Lakes earthquake sequence define a complex zone of faulting along the southern boundary of the Long Valley caldera, and beneath the mountains to the south. The 1980 activity is almost completely contained between the Hilton Creek Fault and a southward projection of the Hartley Springs Fault.

Earthquakes along the southern caldera boundary defines a complex zone of faulting. A well-defined WNW zone dips steeply to the NE and extends from Crowley Lake to the vicinity of Casa Diablo Hot Springs. Clustering of epicenters in the vicinity of Convict Creek Moraine may be related to intersecting fractures. West of the Convict Creek Moraine the activity appears correlative with a fault mapped along the caldera boundary by Rinehart and Ross (1964).

Beneath the mountains south of the caldera, two NNE trending zones of epicenters are observed. The southeastern zone is the most clearly defined and is vertical to a depth of approximately 10 km. This trend occurs beneath the area where Mayo (1937) found anomalous swarms of steeply dipping joints striking N10-20E. Figure 5 shows rose diagrams of steeply dipping joints from Mayo (1937) in four quadrants centered on the south central epicentral area. Note the predominance of joints striking N10-20E in the southeastern quadrant. Figure 19 shows a rose diagram of nodal planes for events with depths less than 9 km from Vetter and Ryall (1983). There is excellent agreement between the NNE nodal planes, the trend of epicenters and the strike of joints as mapped by Mayo (1937). This supports the evidence for the existence of left-lateral strike-slip faulting on vertical planes striking NNE to a depth of approximatly 9-10 km.

Several workers have noted a correspondence between the strike of joints in the crystalline bedrock within the ranges and the strike of the rangefront faults. The predominance of joints with the same strike as that of aftershock trends and nodal planes indicates a causal relationship between the earthquakes and jointing. Many of the joints in the Sierras show measurable displacement and NNE striking fractures exhibiting left-lateral displacement occur near the southern end of the epicentral area (Lockwood and Moore, 1979). In addition NNE striking left-lateral faults which offset Cretaceous intrusives occur in the northeast corner of the Mt. Abbot quadrangle (Lockwood and Lydon, 1975).

While no active faults have been identified from surface mapping within the mountain block south of the caldera, it appears that the NNE structures responsible for some of the seismicity have surface expressions in these joints or microfaults. Whether a particular set of microfaults can be associated with a NNE trending aftershock zone is yet unknown.

The NNE-striking left-lateral faults are either young features being formed in the present tectonic environment or older structures reactivated by the present stress field. Structural inheritance of preexisting planes of weakness by rangefront faults was suggested by Mayo (1941). It is interesting to note, however, that the NNE trend is roughly consistent with planes of maximum shear stress in the present stress regime (Vetter and Ryall, 1983).

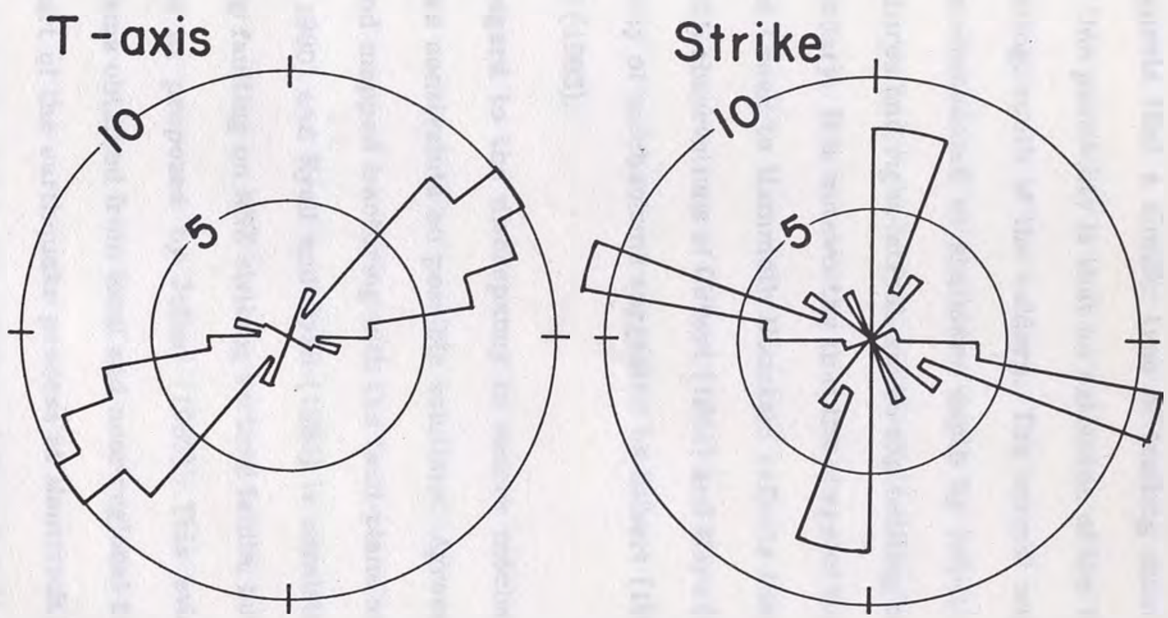

Figure 19. Rose diagram of nodal planes for events shallower than 9 km and T-axes computed from focal mechanisms, from Vetter and Ryall, (1983).

As stated above, the hypocentral zone is bounded on the southwest by an east-dipping plane that is on strike with the Hartley Springs fault, and the deepest events occur in a narrow zone to the east which parallels the Hilton Creek fault. This boundary of the hypocentral zone, parallel to rangefront structures suggests that a similar type of faulting must playing some part in the activity. One possibility is that an extension of the Hartley Springs fault exists, or is forming, south of the caldera. The normal and oblique faulting at depth may be accomodated at shallower depth by left-lateral strike-slip faulting on NNE fractures and right-lateral, strike-slip faulting on WNW faults along the caldera boundary. It is noteworthy that the shape of the entire Rock Creek Salient from Pine Creek to Mammoth Mountain reflects these two trends. This is consistent with observations of Gilbert (1941) and Mayo (1937, 1941) as well as depth dependency of mechanisms suggested by Gilbert (1941) and observed by Vetter and Ryall (1983).

In regard to the discrepancy in source mechanisms, the data presented offer some constraints on possible solutions. Agreement of the NNE epicentral trends and mapped fracturing with the fault-plane solutions of Cramer and Toppozada (1980) and Ryall and Ryall (1980) is consistent with shallow left-lateral strike-slip faulting on NNE striking vertical faults, but not with NW-striking vertical dikes as proposed by Julian (1983). This evidence indicates that focal mechanisms obtained from local and near-regional first-motions are representative of part of the earthquake process at Mammoth Lakes, with relatively small strike-slip events on vertical planes triggering larger events on faults of a different orientation as suggested by Wallace (1984). While there is evidence for magmatic activity, and dike injection may certainly be an integral part of the tectonic process (Lachenbruch and Sass, 1978), there is strong evidence for the

As stated above, the hypocentral zone is bounded on the southwest by an east-dipping plane that is on strike with the Hartley Springs fault, and the deepest events occur in a narrow zone to the east which parallels the Hilton Creek fault. This boundary of the hypocentral zone, parallel to rangefront structures suggests that a similar type of faulting must playing some part in the activity. One possibility is that an extension of the Hartley Springs fault exists, or is forming, south of the caldera. The normal and oblique faulting at depth may be accomodated at shallower depth by left-lateral strike-slip faulting on NNE fractures and right-lateral, strike-slip faulting on WNW faults along the caldera boundary. It is noteworthy that the shape of the entire Rock Creek Salient from Pine Creek to Mammoth Mountain reflects these two trends. This is consistent with observations of Gilbert (1941) and Mayo (1937, 1941) as well as depth dependency of mechanisms suggested by Gilbert (1941) and observed by Vetter and Ryall (1983).

In regard to the discrepancy in source mechanisms, the data presented offer some constraints on possible solutions. Agreement of the NNE epicentral trends and mapped fracturing with the fault-plane solutions of Cramer and Toppozada (1980) and Ryall and Ryall (1980) is consistent with shallow left-lateral strike-slip faulting on NNE striking vertical faults, but not with NW-striking vertical dikes as proposed by Julian (1983). This evidence indicates that focal mechanisms obtained from local and near-regional first-motions are representative of part of the earthquake process at Mammoth Lakes, which may involve relatively small strike-slip events on vertical planes triggering larger events on faults of a different orientation as suggested by Wallace (1984). While there is evidence for magmatic activity, and dike injection may certainly be an integral part of the tectonic process (Lachenbruch and Sass, 1978), there is strong evidence for the involvement of left-lateral strike- slip displacement on NNE striking vertical faults.

Chapter 4.

Seismicity in the Mono Basin - Excelsior Mountain Zone

Introduction

Beginning on 29 June 1980, an earthquake swarm began in the Adobe Hills area east of Mono Lake. The activity was observed to migrate to the northeast with time involving distinct clusters of activity in the Adobe Hills, Huntoon Valley Teels Marsh, and Luning, Nevada areas. Figure 1 shows the seismicity occuring from 1978 to 1983 along with faults from Stewart and Carlson (1978).

Geology

The seismicity occurs within the Mono Basin - Excelsior Mountain Zone (MBEMZ), a broad zone of predominantly left- lateral movement on faults striking N60E (Gilbert *et al.* 1968). The 1934 M-6 1/4 Excelsior Mountain earthquake occured within this zone and produced left-lateral oblique surface rupture (Callahan and Gianella, 1935). The western portion of the MBEMZ in the vicinity of the Adobe Hills and Huntoon Valley is termed a "structural knee" by Gilbert *et al.* (1968) This occurs where the strike of faulting changes abrubtly from the NNW trending faults along the west side of the White Mountains to the ENE faults of the MBEMZ. Within this zone numerous small grabens have formed along NNE striking normal faults.

Seismicity

Historically, the Excelsior Mountain area has had an anomalously high level of seismicity. Results of a study by Ryall and Priestley (1975) suggested that in this area the high degree of crustal fracturing results in strain release by a continuing series of small to moderate earthquakes and fault creep.

The earthquakes used in this study are from the University of Nevada Seismological Laboratory earthquake catalog (Smith and Ryall, 1981). The earthquakes were located using Hypo71r algorithm (Lee and Lahr, 1975), with a velocity model consisting of a 28 km thick crustal layer with P velocity of 6.0 km/sec over a half space with a P velocity of 7.85 km/sec.

Figure 20 shows that three earthquake swarms south of the Excelsior Mountains fall nearly on a straight line trending N60E. Individual swarms and, in particular, the Teels Marsh activity, exhibit elongation in this direction. Focal mechanisms determined by Vetter and Ryall (1983) have nodal planes in good agreement with the epicenter line-ups and are consistent with left-lateral strike-slip faulting on vertical faults striking N60E. The activity at the south end of Huntoon Valley appears to be consistant with the intersection of faults in the "structural knee".

It is important to note that T-axes determined from the focal mechanisms of Vetter and Ryall (1983) are consistant with the geologic structure and trend in a NW-SE direction typical of T-axes for the Basin and Range to the east. Thus, a 50 degree rotation of the extension axis occurs over approximately 30 km between the Mammoth Lakes area and the Adobe Hills area.

Figure 21 is a time-distance plot showing the seismicity occurring between January 1979 and December 1982 in the MBEMZ and in the Mammoth Lakes area. The activity has been projected onto a distance axis in the N30E direction. This

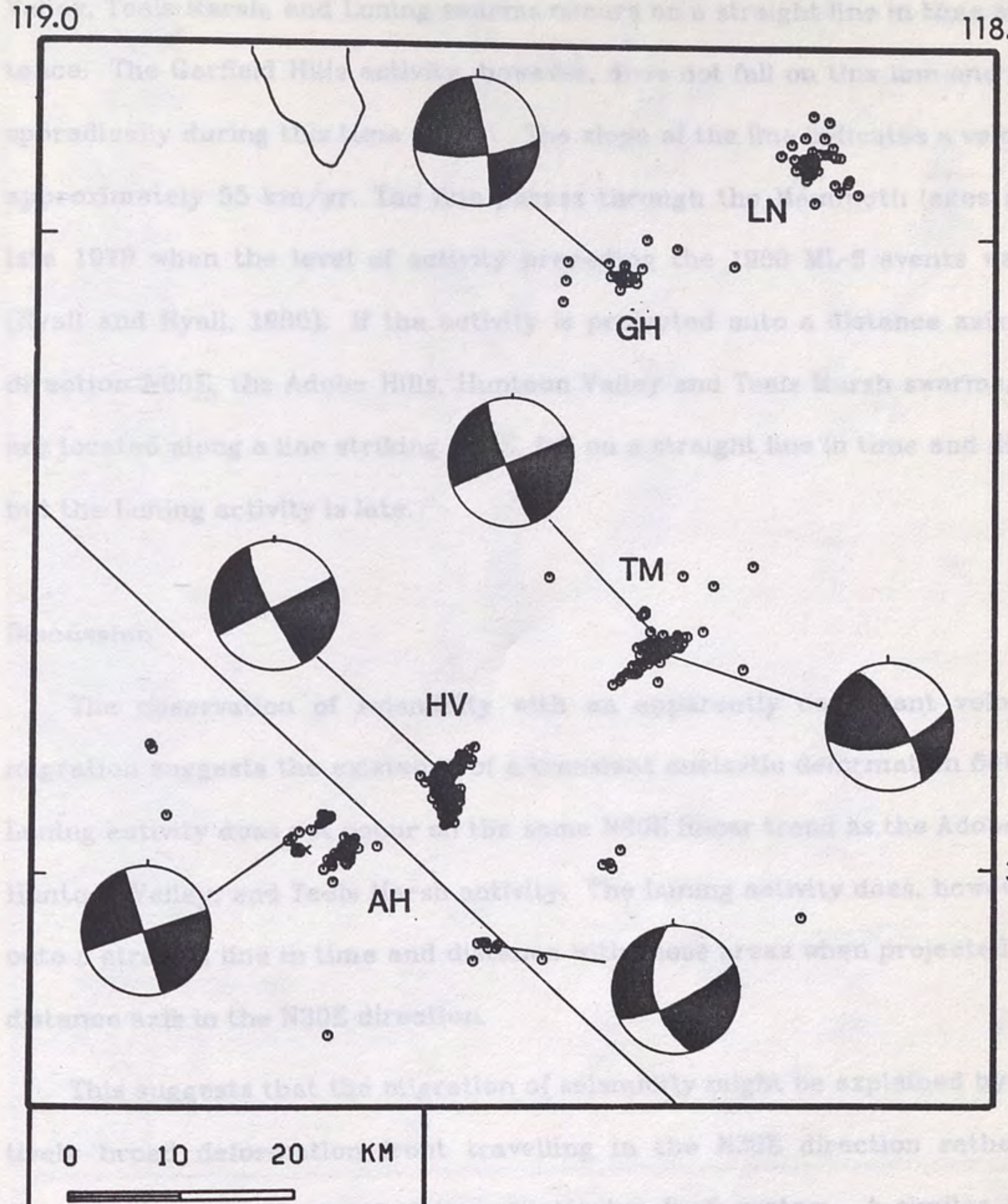

Figure 20. Epicenters of earthquakes in the MBEMZ for the time period June 1980 to Feb. 1982. Focal mechanisms for selected events from U. Vetter. AH -- Adobe Hills; HV -- Huntoon Valley; TM -- Teels Marsh; GH -- Garfield Hills; LN -- Luning Nev.

direction is approximately the direction of maximum horizontal compressive stress in the Basin and Range. The onset of activity in the Adobe Hills, Huntoon Valley, Teels Marsh, and Luning swarms occurs on a straight line in time and distance. The Garfield Hills activity, however, does not fall on this line and occurs sporadically during this time period. The slope of the line indicates a velocity of approximately 55 km/yr. The line passes through the Mammoth lakes area in late 1979 when the level of activity preceding the 1980 ML-6 events was high (Ryall and Ryall, 1980). If the activity is projected onto a distance axis in the direction N60E, the Adobe Hills, Huntoon Valley and Teels Marsh swarms, which are located along a line striking N60E, fall on a straight line in time and distance but the Luning activity is late.

Discussion

The observation of seismicity with an apparently consistant velocity of migration suggests the existence of a transient anelastic deformation field. The Luning activity does not occur on the same N60E linear trend as the Adobe Hills , Huntoon Valley, and Teels Marsh activity. The Luning activity does, however, fall onto a straight line in time and distance with these areas when projected onto a distance axis in the N30E direction.

This suggests that the migration of seismicity might be explained by a relatively broad deformation front travelling in the N30E direction rather than strain propagation restricted to a particular fault system. A similar type of deformation front was hypothesized by Scholz (1977) as a possible explanation for migrating seismicity that led to the successful prediction of the 1975 M=7.3 Haicheng, China earthquake. Scholz suggested the existence of a broad deformation front which migrates in the crust and triggers areas of high seismic

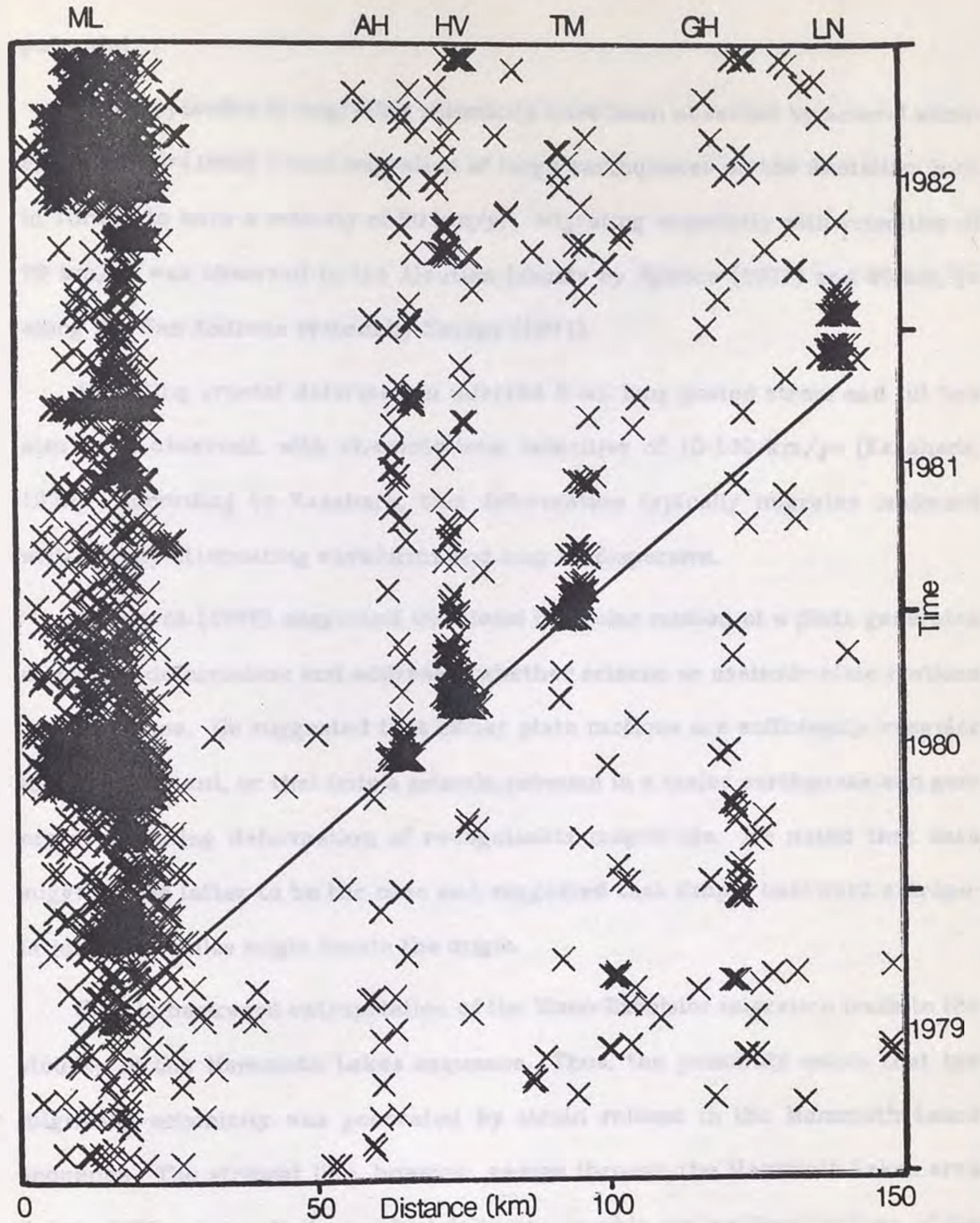

Figure 21. Time-distance plot with earthquakes projected onto a distance axis in the N30E-S30W direction between Mammoth Lakes Ca. and Luning Nev. ML -- Mammoth Lakes; AH -- Adobe Hills; HV -- Huntoon Valley; TM -- Teels Marsh; GH -- Garfield Hills; LN -- Luning Nev.

potential.

Other episodes of migrating seismicity have been observed by several workers. Richter (1958) noted migration of large earthquakes on the Anatolian fault in Turkey to have a velocity of 80 km/yr. Migrating seismicity with velocities of 70 km/yr was observed in the Aleutian Islands by Spence (1977) and 60 km/yr along the San Andreas system by Savage (1971).

Migrating crustal deformation inferred from long period strain and tilt has also been observed, with characteristic velocities of 10-100 km/yr (Kasahara, 1979). According to Kasahara, this deformation typically migrates landward with rapidly attenuating waveforms and may be dispersive.

Kasahara (1979) suggested that local irregular motion of a plate generates migrating deformation and addresses whether seismic or aseismic plate motions are the cause. He suggested that either plate motions are sufficiently irregular and intermittant, or that only a seismic rebound in a major earthquake can generate migrating deformation of recognizable magnitude. He noted that data suggests the latter to be the case and suggested that simple backward extrapolation of the pulse might locate the origin.

Simple backward extrapolation of the Mono-Excelsior migration leads to the vicinity of the Mammoth Lakes sequence. Thus, the possiblity exists that the migrating seismicity was generated by strain release in the Mammoth Lakes sequence. The straight line, however, passes through the Mammoth Lakes area in late 1979, when activity was high but considerably earlier than the time of the greatest seismic strain release. Savage *et al.* (1981) observed no anomalous deformation from trilateration data between 1975 and July 1979 and state that if an observable deformation anomaly occurred prior to the 1980 sequence, it must have happened after mid-July 1979.

Another possible explanation is that the migration was initiated at the time in the Fall of 1978 when, according to a news item in EOS (1979, Vol 60, No. 431), laser ranging measurements in Southern California showed a change in secular strain from north-south compression to east-west extension. There was also a general increase in seismicity over the entire California region during 1979 and 1980 and over the entire SNGBZ (Ryall and Ryall 1980).

Summary

Locations of earthquake swarms in the MBEMZ between 1980 and 1981 are consistant with focal mechanisms determined by Vetter and Ryall (1983) and indicate left-lateral strike-slip faulting on steeply dipping faults striking N60E.

Migration of seismicity to the northeast with time suggests the possibility of a transient anelastic deformation pulse travelling in the direction of maximum horizontal compressive stress (N30E) which triggered earthquake swarms in areas of high seismic potential and/or favorable fault geometry.

The deformation pulse inferred from the observation of migrating seismicity seems best explained by the model of a deformation front such as that proposed by Scholz (1977) for the 1975 Haicheng earthquake. This model seems plausible due to the fact that earthquake swarms, which do not fall on the same linear trend in space, fall on a straight line in time and space when projected onto a distance axis in the direction of maximum horizontal compressive stress.

The inferred pulse could have been triggered by elastic rebound from the 1980 Mammoth Lakes Sequence but more likely was associated with a period of increased activity in late 1979. Another possible explanation is that the inferred pulse was initiated during an episodic change in secular strain which appears to have occurred in late 1978, and which coincided with a general increase in seismic activity in the California-Nevada region.

References

Aki, K., Evidence for magma intrusion during the Mammoth Lakes earthquakes of May, 1980 and implications of the absence of volcanic (harmonic)tremor, submitted to *Jour. Geophys. Res.*, 1984.

Bailey, R. A., Other potential eruption centers in California: Long Valley-Mono Lake, Coso, and Clear Lake volcanic fields, *California Div. Mines Geol. Spec. Pub. 63*, 17-28, 1982.

Bailey, R. A., Dalymple, G. B. and Lanphere, M. A., Volcanism, structure and geochronology of Long Valley caldera, Mono County, California, *Jour. Geophys. Res.*, *81*, 725-744, 1976.

Barker, J. S., and Langston, C. A., A teleseismic body wave analysis of the May 1980 Mammoth Lakes, California, earthquakes, *Bull. Seismol. Soc. Am.*, *73*, 1983.

Bateman, P. C., Geology and tungsten mineralization of the Bishop District, California, *U.S. Geol. Surv. Prof. Pap. 470*, 1965, 208p.

Bateman, P. C. and Merriam, C. W., Geologic map of the Owens Valley region, California, in Jahns, R. H., ed., Geology of southern California, *Cal. Div. Mines Geol. Bull. 170*, 1954.

Bell, E. J., and Slemmons, D. B., Recent crustal movements in the central Sierra Nevada-Walker Lane region of California-Nevada: Part 2, The Pyramid Lake right-slip fault zone segment of the Walker Lane, *Tectonophysics*, *52*, 571-583, 1979.

Benioff, V. H., and Gutenburg, B., The Mammoth "earthquake fault" and related features, *Bull. Seismol. Soc. Am.*, *29*, *(2)*, 333-340, 1939.

Byerly, P., Comment on "The Sierra Nevada in light of isostasy", by Andrew C. Lawson, *Bull. Geol. Soc. Am. 48*, 2025-2031, 1938.

Callahan, E., and Gianella, V. P., The earthquake of January 30, 1934 at Excelsior Mountains, Nevada, *Bull. Seismol. Soc. Am.*, *25*, 161-168, 1935.

Carver, G. A., Quaternary tectonism and surface faulting in the Owens Lake basin, California, *Mackay School of Mines, Tech. Rpt.*, *AT-2*, 103pp, 1970.

Chelikowsky, J. R., Tectonics of the rhyolite in the Mammoth embayment, California, *Jour. Geol. 48*, 421-435, 1940

Clark, M. M., and Gillesbie, A. R., Record of Late Quaternary faulting along the Hilton Creek fault in the Sierra Nevada, California, *Earthquake Notes 52 (1)*, 46, 1981, [abstract].

Clark, M. M., Yount, J. C., Vaughan, P. R., and Zepeda, R. L., Map showing surface ruptures associated with the Mammoth Lakes, California, earthquakes of May 1980, *U.S. Geol. Surv. Map MF-1396*, 1982

Cramer, C. H., and Toppozada, T. R., A seismological study of the May 1980 and earlier earthquake activity near Mammoth Lakes, California, *Calif. Div. Mines Geol. Spec. Rep., 150*, 91-130, 1980.

Eaton, J. P., Crustal structure in Nortern and Central California from seismic evidence, in Bailey, E. H. ed. Geology of Northern California : *Calif. Div. Mines Geol. Bull. 190*,, 419-426, 1966.

Ekstrom, G., Evidence for source complexities of 1980 Mammoth Lakes earthquakes, *EOS, Trans. Am. Geophys. Un., 64*, 262, 1983.

Ekstrom, G., and Dziewonski, A. M., Moment tensor solutions of Mammoth Lakes earthquakes, *EOS, Trans. Am. Geophys. Un., 64*, 262, 1983 [abstract].

Geiger, L., Probability method for the determination of earthquake epicenters from the arrival time only, (translated from Geiger's 1910 German article), *Bulletin of St. Louis University, 8 (1)*, 56-71, 1912.

Gilbert, C. M., Late Tertiary geology southeast of Mono Lake, California, *Bull. Geol. Soc. Am., 52*, 781-816, 1941.

Gilbert, C. M., Christensen, M. N., Al-Rawi, Y. T., and Lajoie, K. R., Structural and volcanic history of Mono Basin, California-Nevada, *Geol. Soc. Am. Memoir 116*, 275-329, 1968.

Given, J. W., Wallace T. C., and Kanamori, H., Teleseismic analysis of the 1980 Mammoth Lakes earthquake sequence, *Bull. Seismol. Soc. Am., 72*, 1093-1109, 1982.

Hill, D. P., Structure of Long Valley caldera from a seismic refraction experiment, *Jour. Geophys. Res., 70*, 745-753, 1976.

Hulin, C. D., Subsequent faulting in the Great Basin, *Bull. Geol. Soc. Am. 42*, 307, 1931 [abstract].

Julian, B. R., Evidence for dyke intrusion earthquake mechanisms near Long Valley caldera, California, *Nature, 303*, 323-325, 1983.

Kasahara, Keichi, Migration of crustal deformation, *Tectonophysics 52*, 329-341, 1979.

Knopoff, L. and Randall, M. J., The compensated linear-vector dipole: a possible mechanism for deep earthquakes, *Jour. Geophys. Res. 75*, 4957-4963, 1970.

Lachenbruch, A. H. and Sass, J. H., Models of an extending lithosphere and heat flow in the Basin and Range province, in Cenozoic tectonics and regional tectonics of the western Cordillera, R. B. Smith and G. P. Eaton, eds., *Geol. Soc. America Memoir 152*, 209-250, 1978.

Lee, W. H. K. and Lahr, J.C., HYPO71: a computer program for determining hypocenter, magnitude and first motion pattern of local earthquakes, *U. S. Geol. Survey, Open-File Rept. 75-311*, 113 pp., 1975.

Lide, C. S., and Ryall, A. S., Relationship of aftershocks locations and mechanisms of the May, 1980 Mammoth Lakes earthquakes, *Active Tectonic and Magmatic Processes in Long Valley Caldera, U. S. Geol. Survey Open-File Rept.*, 1984.

Lockwood, J. P., and Lydon, P. A., Geologic map of the Mount Abbot quadrangle, central Sierra Nevada, California, *U. S. Geol. Survey, Map GQ-1155*, 1975.

Lockwood, J. P. and Moore, J. G., Regional extension of the Sierra Nevada, California, on conjugate microfault sets, *Jour. Geophys. Res.*, *84*, 6041-6049, 1979.

Mayo, E. B., Sierra Nevada pluton and crustal movement, *Jour. Geol.*, *45*, 169-192, 1937.

Mayo, E. B., Deformation in the interval Mt.Lyell-Mt. Whitney, California, *Geol. Soc.Am. Bull. 52*, 1001-1084, 1941.

Miller C. D., Holocene eruptions at the Inyo Volcanic chain, California -- implications for possible eruptions in Long Valley caldera, *Active Tectonic and Magmatic Processes in Long Valley Caldera, U. S. Geol. Survey Open-File Rept.*, 1984.

Mogi, K., Migration of seismic activity, *Bull. Earthquake Res. Inst.*, *46*, 53-74, 1968.

Prodehl, Claus, Crustal Structure of the western United States, *U. S. Geol. Surv. Prof. Paper 1034*, 1979.

Putnam, W. C., Origin of Rock Creek and Owens River Gorges, Mono County, California, *Univ. Calif. Publ. in Geol. Sci. 34*, 221-280, 1960.

Putnam, W. C., Late Cenozoic geology of McGee Mountain, Mono County, California, *Univ. Calif.Publ. in Geol.Sci. 34*, 1962.

Richter, C. F., Elementary Seismology, Freeman and Cooper, San Francisco, California, 611-616, 1958.

Rinehart, C. D. and Ross, D. C., Geology of the Casa Diablo Mountain quadrangle, California,
U. S. Geol. Survey Map GQ-99, 1957.

Rinehart, C. D., and Ross, D. C., Geology and mineral deposits of the Mount Morrison quadrangle, Sierra Nevada, California, *U.S. Geol. Surv. Prof. Paper 385*, 1964.

Rundle, J. B., and Whitcomb, J., A model for deformation in Long Valley, California, 1980-1983, *Active Tectonic and Magmatic Processes in Long Valley Caldera, U. S. Geol. Survey Open-File Rept.*, 1984.

Ryall, A. S. and Priestly, K., Seismicity, secular strain and maximum magnitude in the Excelsior Mountains area, western Nevada and eastern California, *Geol. Soc. Am. Bull.*, *86*, 1585-1592, 1975.

Ryall, A., and Ryall, F., Spatial-temporal variations in seismicity preceding the May, 1980, Mammoth Lakes, California, earthquakes, quakes, *Bull. Seism. Soc. Am.*, *71*, 27-39, 1981a.

Ryall, F., and Ryall, A., Attenuation of P and S waves in a magma chamber in Long Valley caldera, California, *Geophys. Res. Lett. 8*, 557-560, 1981b.

Ryall, A., and Ryall, F., Spasmodic tremor and possible magma injection in Long Valley Caldera, eastern California, *Science*, *219*, 1432-1433,

Ryall, A. S., and Ryall, F. D., Shallow magma bodies related to lithospheric extension in the western Great Basin, western Nevada and eastern California. *Earthquake Notes, 55 (1)*, 11-12, 1984, [abstract]. 1983.

Sanders, C. O. and Slemmons, D. B., Recent crustal movements in the central Sierra Nevada-Walker Lane region of California-Nevada: Part 3, The Olinghouse fault zone, *Tectonophysics*, *52*, 585-597, 1979.

Sanders, C. O., and Ryall, F., Geometry of magma bodies beneath Long Valley California, determined from anomalous earthquake signals, *Geophys. Res. Lett. 10*, 690-692, 1983.

Sanders, C. O., Location and configuration of magma bodies beneath Long Valley, California, determined from anomalous earthquake signals, *Jour. Geophys. Res.*, *89 (B10)*, 8287-8302, 1984.

Savage, J. C., A theory of creep waves propagating along a transform fault, *Jour. Geophys. Res. 76, no. 8*, 1954-1966, 1971.

Savage, J. C., Lisowski, M., Prescott, W. H., and King, N. E., Strain accumulation near the epicenter of the 1978 Bishop and 1980 Mammoth Lakes, California earthquakes, *Bull. Seism. Soc. Am.*, *71*, 465-476, 1981.

Savage, J. C., and Clark, M. M., Magmatic resurgence in Long Valley caldera, California: Possible cause of the 1980 Mammoth Lakes earthquakes, *Science*, *217*, 531-533, 1982.

Savage, J. C., and Cockerham, R. S., Earthquake swarm in Long Valley caldera, California, January 1983: evidence for dike inflation, *Jour. Geophys. Res. 89 (B10)*, 8315-8324, 1984.

Scholz, C. H., A physical interpretation of the Haicheng earthquake prediction, *Nature, 267*, 121-124, 1977.

Sipkin, S. A. and Julian, B. R., Evidence for non-double couple earthquake mechanisms, *EOS, Trans. Am. Geophys. Un., 64*, 262, 1983 [abstract].

Slemmons, D. B., VanWormer, J. D., Bell, E. J., and Silberman, M. L., Recent crustal movements in the Sierra Nevada-Walker Lane region of California-Nevada: Part 1, Rate and style of deformation, *Tectonophysics, 52*, 571-583, 1979.

Smith, G. M., and Ryall, F. D., eds. Bulletin of the Seismological Laboratory, *Mackay School of Mines*, 50pp, 1982.

Sorey, M. L., Lewis, R. E., and Olmstead, F. H., The hydrothermal system of Long Valley Caldera, California, *US Geol. Survey Prof. Paper 1044-A*, 60 pp., 1978.

Spence, W., The Aleutian arc: tectonic blocks, episodic subduction, strain diffusion, and magma generation, *Jour. Geophys. Res. 82 (2)*, 213-230, 1977.

Stewart, J. H., Basin and Range structure -- a system of horsts and grabens produced by deep seated extension, *Geol. Soc. Am. Bull. 82*, 1019-1044, 1971.

Stewart, J. H., Geology of Nevada, *Nev. Bur. Mines Spec. Pub. 4*, 136pp, 1980.

Stewart, J. H., and Carlson J. E., Geologic map of Nevada, *U. S. Geol. Survey Map MF-930*, 1978.

Strand, R. G., Geologic map of California, Olaf P. Jenkins edition, Mariposa sheet, *Cal. Div. Mines Geol.*, 1967.

Taylor, G. C., and Bryant W. A., Surface rupture associated with the Mammoth Lakes earthquakes of 25 and 27 May, 1980, *Calif. Div. Mines Geol. Spec. Rep., 150*, 49-67, 1980.

Thompson, G. A., and Burke, D. B, Regional geophysics of the Basin and Range province, *Ann. Rev. Earth and Planetary Sci., 2*, 213-238, 1974.

Univ. Calif., Berkeley, *Bull. Seismogr. Stations, 50*, 87 pp., 1980.

U. S. Geol. Survey, *Volcano Hazards Assessed for California's Long Valley-Mono Lake Area*, prcss rclcasc, 5 pp., 1982.

Vetter, U. R. and Ryall A. S., Systematic change of focal mechanisms with depth in the western Great Basin, *Jour. Geophys. Res., 88*, 8237-8250, 1983.a

Wadati, K., Shallow and deep earthquakes, *Geophysical Magazine* (Tokyo) 1, 162-202, 1928.

Wallace, T. C., Given, J., and Kanamori, H., A discrepancy between long- and short-period mechanisms of earthquakes near the Long Valley caldera, *Geophys. Res. Lett. 9,*, 1131-1134, 1982.

Wallace, T. C., *Long Period Regional Body Waves*, Calif. Inst. Technology, PhD Dissertation, 180 pp., 1983.

Wallace, T. C., A re-examination of the moment tensor solutions of the 1980 Mammoth Lakes earthquakes, *Active Tectonic and Magmatic Processes in Long Valley Caldera, US Geol. Survey open-file Rept.*, 1984.

Appendix A
List of Earthquakes.

Date	Origin	Latitude	Longitude	Depth	# Sta	RMS
05/25/80	16:33:44.70	37N35.50	118W50.05	4.85	6	0.07
05/27/80	14:50:56.94	37N28.82	118W48.74	11.85	7	0.03
05/28/80	09:02:36.43	37N37.65	118W61.04	6.97	8	0.06
05/28/80	09:19:46.53	37N29.31	118W50.95	6.61	7	0.05
05/28/80	09:20:30.69	37N33.02	118W47.21	6.57	7	0.04
05/28/80	10:13:02.77	37N28.56	118W50.30	10.03	8	0.03
05/28/80	13:27:38.69	37N35.20	118W49.18	6.23	8	0.02
05/28/80	14:06:30.14	37N30.84	118W47.70	3.79	10	0.07
05/28/80	14:18:22.37	37N27.25	118W51.55	4.63	8	0.06
05/28/80	14:47:32.12	37N31.35	118W49.06	11.06	8	0.05
05/28/80	15:42:39.25	37N28.73	118W49.03	7.03	8	0.06
05/28/80	17:28:23.81	37N33.99	118W53.17	4.41	8	0.05
05/28/80	17:32:21.56	37N32.76	118W53.51	3.78	9	0.03
05/28/80	18:03:15.20	37N36.84	118W53.03	5.75	8	0.05
05/28/80	18:35:09.50	37N29.92	118W48.11	8.18	8	0.04
05/28/80	18:37:18.72	37N33.34	118W53.59	0.87	10	0.04
05/28/80	19:00:00.95	37N30.34	118W50.50	8.56	8	0.03
05/28/80	19:26:40.83	37N30.64	118W48.51	9.97	8	0.03
05/28/80	21:02:00.59	37N29.32	118W48.69	9.16	6	0.04
05/28/80	21:54:10.82	37N32.03	118W48.80	8.86	8	0.06
05/28/80	23:07:19.27	37N35.73	118W47.89	3.33	8	0.02
05/28/80	23:10:06.66	37N37.53	118W51.78	6.29	6	0.05
05/28/80	23:17:15.96	37N33.42	118W52.50	3.38	8	0.04
05/28/80	23:50:19.83	37N32.14	118W49.24	8.98	8	0.03
05/29/80	04:17:41.48	37N29.85	118W49.83	9.57	9	0.03
05/29/80	04:18:52.64	37N32.16	118W49.55	10.19	9	0.04
05/29/80	04:33:35.31	37N29.83	118W49.73	9.31	9	0.03
05/29/80	04:42:29.79	37N35.85	118W46.53	4.93	9	0.02
05/29/80	05:32:04.62	37N37.47	118W51.80	5.88	9	0.04
05/29/80	07:32:21.36	37N29.08	118W49.04	3.05	9	0.05
05/29/80	09:34:26.96	37N38.23	118W53.20	6.74	9	0.05
05/29/80	09:47:37.97	37N34.62	118W51.07	8.21	9	0.03
05/29/80	10:39:37.44	37N37.11	118W51.22	4.96	9	0.07
05/29/80	11:03:57.56	37N28.86	118W49.10	3.04	6	0.07
05/29/80	11:33:24.22	37N33.10	118W45.60	4.10	6	0.08
05/29/80	11:59:18.45	37N35.43	118W49.26	6.59	9	0.02
05/29/80	13:33:43.49	37N37.94	118W50.98	5.88	6	0.05
05/29/80	13:52:00.04	37N36.11	118W53.49	1.58	9	0.09
05/29/80	14:00:26.15	37N31.45	118W50.06	9.88	9	0.03
05/29/80	15:16:05.16	37N34.81	118W49.20	4.00	11	0.04
05/29/80	15:20:34.19	37N30.04	118W50.67	11.04	9	0.03
05/29/80	16:01:44.85	37N36.98	118W53.16	6.47	8	0.05
05/29/80	16:14:08.36	37N36.84	118W53.58	5.04	9	0.05
05/29/80	16:56:56.82	37N29.91	118W52.60	2.05	10	0.06
05/29/80	17:21:01.39	37N30.46	118W50.81	2.20	10	0.04

Appendix A
(continued)

Date	Origin	Latitude	Longitude	Depth	# Sta	RMS
05/29/80	18:35:15.46	37N33.54	118W52.12	6.43	9	0.02
05/29/80	17:28:30.27	37N30.20	118W51.03	0.95	9	0.05
05/29/80	18:24:44.36	37N38.09	118W51.25	4.91	9	0.05
05/29/80	18:55:09.17	37N35.70	118W47.78	4.60	11	0.03
05/29/80	19:23:58.08	37N36.87	118W52.84	6.30	8	0.03
05/29/80	20:01:16.39	37N36.84	118W52.68	5.97	9	0.05
05/29/80	20:47:00.51	37N36.99	118W53.00	7.22	9	0.04
05/29/80	22:32:24.22	37N31.59	118W52.46	2.47	8	0.03
05/29/80	22:35:39.39	37N37.66	118W57.15	5.32	9	0.07
05/29/80	22:40:57.92	37N32.09	118W50.29	3.08	9	0.03
05/29/80	22:52:41.66	37N31.62	118W48.46	0.66	7	0.05
05/29/80	23:06:04.29	37N33.67	118W53.10	0.40	9	0.05
05/29/80	23:13:37.33	37N27.52	118W49.63	2.36	9	0.05
05/29/80	23:14:06.04	37N37.41	118W52.73	5.83	9	0.04
05/30/80	00:10:32.55	37N36.78	118W48.30	6.57	9	0.03
05/30/80	00:25:29.69	37N33.77	118W50.14	2.53	8	0.03
05/30/80	00:46:18.20	37N37.06	118W50.89	9.99	8	0.03
05/30/80	00:46:42.28	37N28.57	118W48.95	5.83	9	0.05
05/30/80	00:54:58.72	37N37.28	118W52.11	5.36	9	0.05
05/30/80	01:09:59.31	37N36.69	118W53.62	1.89	7	0.07
05/30/80	01:19:09.10	37N31.95	118W45.39	0.05	8	0.06
05/30/80	01:19:32.61	37N34.52	118W45.80	3.48	9	0.06
05/30/80	01:25:55.39	37N36.79	118W51.56	3.46	9	0.07
05/30/80	01:30:07.74	37N34.15	118W53.43	0.35	9	0.06
05/30/80	01:52:00.22	37N28.05	118W49.21	5.79	9	0.05
05/30/80	01:58:03.62	37N37.18	118W51.91	5.10	9	0.04
05/30/80	02:06:00.13	37N32.61	118W49.12	10.39	8	0.02
05/30/80	02:12:19.17	37N29.15	118W48.80	8.29	9	0.04
05/30/80	02:25:54.99	37N35.37	118W47.06	5.34	9	0.02
05/30/80	03:04:54.49	37N28.48	118W51.12	5.32	9	0.06
05/30/80	04:57:31.25	37N28.65	118W50.65	6.37	9	0.05
05/30/80	05:19:00.68	37N30.36	118W50.28	8.83	9	0.03
05/30/80	05:19:28.70	37N29.15	118W48.77	3.63	9	0.07
05/30/80	05:22:43.14	37N35.58	118W48.74	6.12	9	0.02
05/30/80	05:28:58.98	37N34.26	118W53.43	0.89	9	0.05
05/30/80	05:30:37.46	37N34.23	118W53.46	2.21	8	0.03
05/30/80	05:42:54.32	37N35.59	118W48.69	5.77	9	0.03
05/30/80	05:51:52.74	37N34.99	118W45.65	0.04	9	0.04
05/30/80	05:55:33.70	37N30.09	118W48.33	7.23	9	0.06
05/30/80	05:58:45.72	37N37.51	118W51.45	7.09	9	0.03
05/30/80	06:05:10.53	37N28.84	118W48.78	5.44	9	0.04
05/30/80	06:29:27.99	37N36.69	118W52.46	4.82	6	0.07
05/30/80	06:39:07.37	37N37.19	118W54.25	4.81	9	0.07
05/30/80	06:52:04.66	37N33.59	118W53.53	1.86	9	0.08
05/30/80	07:08:21.86	37N28.85	118W49.14	2.94	6	0.06

Appendix A
(continued)

Date	Origin	Latitude	Longitude	Depth	# Sta	RMS
05/30/80	07:25:16.01	37N37.54	118W51.67	6.85	9	0.03
05/30/80	07:12:39.39	37N31.92	118W50.40	2.17	9	0.03
05/30/80	07:21:40.30	37N34.27	118W53.24	2.34	9	0.10
05/30/80	07:28:13.24	37N34.88	118W45.58	0.83	9	0.04
05/30/80	07:42:23.06	37N31.64	118W48.98	10.82	9	0.03
05/30/80	07:52:05.90	37N34.79	118W49.19	2.20	9	0.02
05/30/80	09:19:17.14	37N28.60	118W51.22	4.29	9	0.04
05/30/80	09:28:21.84	37N33.27	118W50.75	7.92	9	0.03
05/30/80	10:26:56.92	37N36.14	118W47.34	6.20	8	0.04
05/30/80	10:30:13.90	37N33.39	118W51.53	8.35	9	0.03
05/30/80	10:30:51.31	37N36.02	118W53.57	2.15	9	0.06
05/30/80	10:46:24.34	37N37.14	118W57.18	4.07	8	0.10
05/30/80	11:14:04.47	37N30.44	118W49.31	10.49	6	0.04
05/30/80	11:30:21.47	37N34.90	118W49.11	6.49	9	0.02
05/30/80	12:00:50.11	37N31.04	118W51.83	4.53	9	0.05
05/30/80	12:01:52.95	37N30.93	118W51.81	4.05	6	0.03
05/30/80	12:53:30.55	37N34.57	118W46.40	3.94	9	0.03
05/30/80	12:57:01.93	37N35.39	118W49.73	4.45	9	0.03
05/30/80	13:29:47.02	37N35.63	118W47.72	5.61	8	0.02
05/30/80	13:32:50.36	37N37.51	118W51.96	4.28	9	0.06
05/30/80	13:38:51.42	37N37.59	118W52.04	4.89	9	0.05
05/30/80	13:40:52.37	37N34.12	118W49.05	3.51	6	0.02
05/30/80	13:49:17.00	37N34.75	118W49.22	4.21	9	0.02
05/30/80	15:04:35.16	37N35.40	118W49.83	4.63	9	0.03
05/30/80	15:05:17.67	37N34.63	118W52.83	1.03	9	0.06
05/30/80	15:23:08.47	37N37.07	118W53.46	6.23	8	0.05
05/30/80	15:32:19.95	37N37.53	118W51.72	7.54	9	0.03
05/30/80	15:41:57.97	37N33.42	118W54.40	1.43	6	0.04
05/30/80	15:49:02.35	37N31.70	118W47.54	4.00	6	0.06
05/30/80	16:03:42.11	37N28.25	118W51.17	5.42	9	0.05
05/30/80	16:48:46.99	37N29.60	118W48.84	12.32	9	0.03
05/30/80	17:05:27.03	37N29.64	118W50.79	6.20	8	0.01
05/30/80	17:41:26.25	37N36.17	118W47.73	6.68	9	0.04
05/30/80	17:42:00.91	37N32.95	118W50.89	7.98	9	0.03
05/30/80	18:15:53.37	37N33.68	118W49.68	0.65	9	0.05
05/30/80	18:28:02.70	37N35.84	118W54.01	0.52	9	0.09
05/30/80	18:28:47.95	37N32.54	118W51.66	5.52	9	0.03
05/30/80	18:36:06.09	37N32.11	118W48.47	0.03	6	0.05
05/30/80	18:43:24.80	37N36.81	118W49.97	5.05	9	0.04
05/30/80	18:43:38.82	37N33.86	118W50.45	8.67	7	0.02
05/30/80	18:49:08.21	37N35.52	118W49.74	4.13	9	0.03
05/30/80	19:12:29.99	37N35.61	118W56.83	2.80	9	0.06
05/30/80	19:49:02.79	37N34.10	118W52.45	5.53	6	0.04
05/30/80	20:30:37.80	37N36.61	118W49.55	6.37	6	0.04
05/30/80	20:36:35.97	37N29.72	118W50.68	4.38	9	0.04

Appendix A
(continued)

Date	Origin	Latitude	Longitude	Depth	# Sta	RMS
05/30/80	22:13:24.62	37N34.24	118W52.46	5.52	9	0.04
05/30/80	20:40:28.04	37N32.52	118W52.72	2.43	8	0.04
05/30/80	21:49:35.54	37N27.94	118W49.36	5.72	9	0.04
05/30/80	23:02:32.56	37N32.24	118W49.96	6.96	6	0.03
05/31/80	00:13:26.34	37N34.17	118W52.79	0.21	9	0.09
05/31/80	00:18:49.08	37N34.24	118W53.19	1.80	9	0.04
05/31/80	00:58:17.81	37N29.57	118W51.01	4.61	7	0.04
05/31/80	01:12:50.44	37N35.69	118W46.80	4.49	9	0.02
05/31/80	01:24:37.28	37N29.56	118W51.22	3.07	9	0.04
05/31/80	01:43:29.56	37N34.23	118W49.36	3.14	9	0.02
05/31/80	02:25:01.32	37N36.03	118W47.39	6.37	9	0.04
05/31/80	05:14:34.69	37N34.59	118W49.67	7.99	10	0.03
05/31/80	05:16:09.86	37N34.71	118W49.67	7.94	10	0.02
05/31/80	05:28:38.18	37N35.70	118W49.93	1.76	10	0.04
05/31/80	06:53:34.27	37N30.19	118W50.74	3.73	10	0.04
05/31/80	08:05:19.62	37N33.08	118W49.72	9.27	10	0.00
05/31/80	08:11:47.55	37N35.69	118W47.39	5.86	10	0.04
05/31/80	08:37:04.68	37N28.11	118W49.25	6.03	10	0.04
05/31/80	10:11:31.06	37N34.95	118W49.10	2.47	10	0.03
05/31/80	10:14:31.08	37N35.14	118W48.98	3.61	8	0.07
05/31/80	13:13:40.60	37N34.81	118W49.32	2.30	12	0.04
05/31/80	13:28:17.11	37N34.52	118W49.33	2.57	9	0.02
05/31/80	13:43:48.79	37N34.49	118W49.43	2.99	10	0.03
05/31/80	14:06:46.12	37N30.43	118W47.21	3.73	10	0.05
05/31/80	14:58:26.52	37N30.44	118W52.26	2.35	10	0.05
05/31/80	15:07:37.12	37N32.42	118W52.09	4.15	8	0.03
05/31/80	15:07:44.16	37N28.64	118W49.18	0.95	7	0.07
05/31/80	15:16:11.76	37N35.67	118W47.40	5.92	6	0.02
05/31/80	15:20:19.77	37N35.59	118W47.05	4.36	10	0.04
05/31/80	15:35:17.89	37N35.45	118W47.37	4.97	7	0.00
05/31/80	18:18:23.27	37N34.14	118W52.22	3.26	9	0.05
05/31/80	18:23:06.97	37N37.08	118W53.93	5.83	9	0.06
05/31/80	19:06:47.95	37N34.36	118W46.48	3.79	11	0.03
05/31/80	19:19:36.32	37N35.17	118W47.62	4.55	8	0.01
05/31/80	19:33:00.72	37N35.66	118W46.71	5.22	9	0.05
05/31/80	19:38:49.79	37N35.76	118W48.13	2.92	9	0.02
05/31/80	19:39:06.67	37N31.25	118W49.83	10.37	8	0.03
05/31/80	19:56:07.33	37N37.33	118W56.14	5.64	10	0.10
05/31/80	20:14:40.49	37N35.68	118W47.06	6.44	10	0.03
05/31/80	23:15:29.28	37N36.41	118W50.15	11.46	10	0.02
06/01/80	00:57:36.98	37N35.63	118W54.70	2.50	10	0.07
06/01/80	05:28:48.38	37N29.02	118W48.65	6.34	10	0.05
06/01/80	06:47:36.54	37N28.40	118W50.81	3.62	12	0.06
06/01/80	07:00:16.63	37N28.81	118W50.85	1.16	11	0.06
06/01/80	07:47:17.50	37N36.41	118W54.81	3.77	10	0.06

Appendix A
(continued)

Date	Origin	Latitude	Longitude	Depth	# Sta	RMS
06/01/80	14:59:05.32	37N36.76	118W54.53	1.89	9	0.10
06/01/80	12:21:00.30	37N35.43	118W47.06	6.02	12	0.04
06/01/80	13:08:23.42	37N35.58	118W48.82	6.04	9	0.03
06/01/80	16:09:50.90	37N31.89	118W45.54	1.63	9	0.10
06/01/80	17:27:24.98	37N34.42	118W46.40	4.53	12	0.07
06/01/80	18:40:59.38	37N33.93	118W49.60	0.14	8	0.01
06/01/80	19:52:03.22	37N34.59	118W53.20	0.21	10	0.04
06/01/80	21:09:47.55	37N33.52	118W52.88	1.86	10	0.07
06/01/80	21:23:07.73	37N35.96	118W54.19	4.75	11	0.06
06/01/80	22:12:47.40	37N35.40	118W46.70	6.19	10	0.02
06/01/80	22:30:22.47	37N37.19	118W52.72	7.45	12	0.03
06/01/80	22:38:15.20	37N37.50	118W56.93	4.12	10	0.09
06/01/80	23:32:21.10	37N31.79	118W45.62	1.90	9	0.08
06/02/80	00:42:32.95	37N29.75	118W48.75	7.92	8	0.07
06/02/80	01:16:16.19	37N36.75	118W52.61	3.00	11	0.08
06/02/80	02:30:15.31	37N33.89	118W53.07	1.37	10	0.05
06/02/80	03:07:45.56	37N33.44	118W52.79	0.88	11	0.04
06/02/80	03:23:30.66	37N28.44	118W49.26	7.56	10	0.05
06/02/80	04:27:52.29	37N27.44	118W51.77	6.99	6	0.05
06/02/80	07:42:55.36	37N36.82	118W48.40	7.45	11	0.04
06/02/80	09:08:30.09	37N36.97	118W53.63	5.13	9	0.07
06/02/80	09:19:03.47	37N34.63	118W50.90	8.14	11	0.02
06/02/80	09:33:30.27	37N37.21	118W54.38	5.69	10	0.06
06/02/80	10:14:40.71	37N35.99	118W49.07	4.42	11	0.03
06/02/80	10:22:20.75	37N35.72	118W54.77	3.93	12	0.06
06/02/80	11:21:43.29	37N35.82	118W48.05	3.69	10	0.02
06/02/80	11:55:38.17	37N37.95	118W52.17	5.02	10	0.08
06/02/80	12:35:11.62	37N32.56	118W51.68	4.21	10	0.02
06/02/80	12:42:30.92	37N27.80	118W49.24	6.44	11	0.05
06/02/80	12:46:33.35	37N36.69	118W52.96	3.82	11	0.09
06/02/80	13:06:44.97	37N36.80	118W50.89	4.96	11	0.05
06/02/80	13:47:32.49	37N36.07	118W54.86	4.96	10	0.06
06/02/80	13:54:14.12	37N28.84	118W49.02	2.87	11	0.05
06/02/80	15:34:36.08	37N35.64	118W47.90	3.75	10	0.03
06/02/80	15:57:03.07	37N30.10	118W48.44	11.06	11	0.03
06/02/80	16:19:04.24	37N36.10	118W54.71	4.20	11	0.07
06/02/80	16:43:29.60	37N34.85	118W45.61	1.81	10	0.04
06/02/80	16:51:02.48	37N31.70	118W48.73	11.34	11	0.03
06/02/80	17:09:51.91	37N36.86	118W51.91	6.02	9	0.03
06/02/80	17:24:41.41	37N36.25	118W50.23	3.65	10	0.03
06/02/80	18:54:07.17	37N38.02	118W53.30	7.49	11	0.05
06/02/80	18:55:46.99	37N34.40	118W49.34	4.02	11	0.02
06/02/80	19:35:23.88	37N35.78	118W54.73	2.74	11	0.07
06/02/80	20:12:31.95	37N34.94	118W45.72	1.18	11	0.05
06/02/80	20:15:12.63	37N36.48	118W52.49	3.41	11	0.06

Appendix A
(continued)

Date	Origin	Latitude	Longitude	Depth	# Sta	RMS
06/02/80	20:37:19.51	37N33.89	118W52.04	3.45	11	0.03
06/02/80	20:16:04.44	37N35.39	118W49.39	5.57	9	0.03
06/02/80	20:34:13.95	37N33.80	118W52.06	4.29	11	0.03
06/02/80	20:38:28.05	37N33.96	118W52.00	3.36	11	0.03
06/02/80	20:58:39.49	37N37.11	118W52.19	4.30	11	0.06
06/02/80	21:58:30.68	37N36.92	118W51.27	8.44	11	0.03
06/02/80	22:49:23.54	37N36.03	118W47.52	7.08	11	0.03
06/02/80	23:18:42.27	37N36.11	118W54.72	5.33	8	0.05
06/02/80	23:20:44.22	37N33.83	118W52.05	3.57	11	0.04
06/02/80	23:53:48.87	37N33.89	118W49.44	3.52	11	0.03
06/03/80	00:39:05.86	37N31.08	118W51.67	3.63	11	0.04
06/03/80	01:44:51.66	37N37.62	118W56.49	3.16	10	0.07
06/03/80	02:57:18.31	37N31.61	118W50.45	4.66	9	0.04
06/03/80	03:30:15.00	37N36.25	118W54.72	4.09	11	0.06
06/03/80	04:07:39.04	37N36.35	118W54.87	4.12	10	0.07
06/03/80	04:12:00.40	37N35.46	118W46.64	5.17	9	0.02
06/03/80	04:27:52.43	37N27.71	118W51.40	6.09	11	0.05
06/03/80	05:21:25.01	37N36.27	118W54.88	3.36	11	0.07
06/03/80	05:54:00.36	37N32.47	118W47.99	11.09	11	0.03
06/03/80	06:18:44.40	37N36.61	118W50.13	5.69	11	0.04
06/03/80	06:39:45.83	37N34.49	118W49.45	5.20	11	0.07
06/03/80	06:56:29.28	37N30.23	118W48.19	12.75	10	0.03
06/03/80	07:05:15.84	37N35.92	118W48.49	5.04	10	0.02
06/03/80	07:05:35.44	37N37.03	118W51.60	5.28	9	0.04
06/03/80	07:23:16.79	37N36.72	118W50.14	5.97	11	0.05
06/03/80	07:24:15.06	37N36.46	118W50.07	4.83	11	0.05
06/03/80	07:32:01.77	37N36.56	118W51.22	3.72	11	0.05
06/03/80	07:32:01.77	37N36.58	118W51.22	3.68	9	0.06
06/03/80	07:45:53.54	37N30.69	118W47.50	0.53	11	0.06
06/03/80	08:19:16.54	37N30.83	118W47.47	1.60	9	0.06
06/03/80	09:24:11.37	37N36.41	118W49.49	5.85	11	0.07
06/03/80	10:10:25.73	37N27.87	118W49.45	12.75	9	0.03
06/03/80	10:22:21.66	37N34.58	118W49.67	4.49	11	0.04
06/03/80	11:15:22.79	37N29.37	118W48.79	3.70	10	0.05
06/03/80	13:00:53.10	37N30.82	118W47.43	1.43	10	0.04
06/03/80	13:12:24.31	37N35.58	118W48.19	2.96	6	0.01
06/03/80	13:12:44.28	37N35.53	118W48.20	3.14	11	0.03
06/03/80	14:32:52.15	37N31.51	118W51.46	5.93	10	0.02
06/03/80	14:48:41.46	37N31.13	118W48.50	11.98	9	0.03
06/03/80	14:56:17.47	37N32.16	118W52.55	1.73	10	0.04
06/03/80	15:37:54.41	37N35.87	118W46.94	0.89	10	0.03
06/03/80	16:29:52.48	37N29.81	118W50.67	3.81	7	0.01
06/03/80	16:44:50.35	37N29.54	118W50.71	4.70	11	0.03
06/03/80	17:10:25.84	37N30.59	118W49.93	2.86	11	0.04
06/03/80	17:34:12.35	37N31.66	118W49.01	12.00	8	0.03

Appendix A
(continued)

Date	Origin	Latitude	Longitude	Depth	# Sta	RMS
06/03/80	19:38:17.40	37N33.63	118W51.51	3.12	8	0.03
06/03/80	18:33:02.12	37N37.40	118W49.82	9.68	8	0.02
06/03/80	20:02:47.75	37N29.03	118W49.00	1.88	11	0.05
06/03/80	20:23:12.52	37N37.75	118W57.08	5.35	11	0.06
06/03/80	20:43:06.88	37N37.86	118W52.12	3.95	10	0.07
06/03/80	20:59:19.59	37N30.88	118W50.32	9.02	11	0.03
06/03/80	23:57:29.48	37N38.33	118W53.81	7.07	11	0.05
06/04/80	02:38:21.88	37N36.50	118W51.22	4.09	12	0.05
06/04/80	08:34:20.42	37N28.60	118W48.84	5.83	13	0.05
06/04/80	13:41:15.21	37N35.60	118W46.88	6.05	9	0.03
06/04/80	19:09:21.74	37N31.85	118W52.60	1.47	12	0.05
06/04/80	21:00:20.17	37N36.24	118W54.63	2.32	9	0.07
06/13/80	21:13:43.32	37N31.30	118W50.12	1.90	9	0.04
06/13/80	23:23:20.08	37N29.47	118W49.00	8.99	11	0.04
06/14/80	03:36:32.80	37N34.12	118W53.20	2.11	9	0.05
06/14/80	05:47:47.84	37N37.09	118W53.76	2.99	10	0.09
06/14/80	07:35:55.38	37N29.96	118W48.65	9.31	10	0.04
06/14/80	08:22:38.80	37N37.14	118W50.87	8.30	6	0.03
06/14/80	11:30:47.15	37N36.56	118W54.13	5.03	8	0.07
06/14/80	13:50:53.87	37N34.15	118W50.34	0.61	8	0.05
06/15/80	10:55:33.95	37N36.11	118W47.44	7.43	9	0.04
06/15/80	16:24:49.72	37N36.39	118W52.53	4.49	9	0.08
06/16/80	08:23:38.81	37N37.14	118W50.93	8.25	6	0.03
06/16/80	13:33:50.07	37N29.07	118W48.90	9.64	9	0.04
06/16/80	14:02:19.62	37N32.19	118W46.59	0.32	9	0.07
06/16/80	21:46:30.64	37N32.41	118W50.07	3.65	9	0.03
06/18/80	18:55:37.85	37N30.69	118W50.62	1.95	9	0.03
06/19/80	14:04:30.26	37N37.47	118W51.20	7.39	9	0.05
06/19/80	17:21:05.51	37N33.45	118W51.00	0.51	9	0.04
06/19/80	22:26:16.86	37N37.30	118W55.54	7.86	9	0.04
06/20/80	15:25:00.26	37N31.70	118W51.48	5.55	9	0.03
06/20/80	16:04:21.38	37N35.10	118W46.50	4.99	9	0.04
06/21/80	19:38:42.97	37N33.29	118W46.60	1.50	8	0.05
06/21/80	22:01:10.05	37N31.62	118W52.70	6.06	10	0.03
06/22/80	04:47:22.06	37N35.21	118W50.21	5.47	8	0.02
06/23/80	00:07:43.53	37N30.64	118W45.49	1.63	8	0.08
06/23/80	05:16:53.00	37N34.96	118W50.34	8.99	9	0.02
06/23/80	06:32:21.77	37N33.83	118W50.03	8.56	9	0.03
06/24/80	21:44:42.19	37N33.61	118W50.30	0.22	9	0.06
06/25/80	05:51:22.85	37N36.78	118W49.50	5.18	8	0.02
06/25/80	19:10:18.13	37N28.40	118W50.97	5.77	8	0.02
06/26/80	00:30:11.00	37N33.45	118W50.99	7.16	8	0.04
06/26/80	05:41:47.25	37N30.17	118W48.81	11.03	8	0.02
06/26/80	09:48:32.46	37N35.37	118W48.95	4.88	8	0.03

Appendix A
(continued)

Date	Origin	Latitude	Longitude	Depth	# Sta	RMS
06/28/80	03:53:01.67	37N34.67	118W49.33	1.83	8	0.04
06/28/80	00:57:34.03	37N34.31	118W49.49	0.85	8	0.03
06/28/80	00:58:42.32	37N34.50	118W49.28	0.43	7	0.05
06/28/80	20:32:36.76	37N37.42	118W51.66	6.35	9	0.07
06/29/80	04:16:13.38	37N31.37	118W49.42	2.20	8	0.05
06/29/80	07:59:10.30	37N36.75	118W49.89	4.96	9	0.04
06/30/80	01:49:14.67	37N36.22	118W55.23	3.83	9	0.10
06/30/80	02:09:44.00	37N28.00	118W49.28	11.84	9	0.03
07/01/80	06:38:13.68	37N34.15	118W49.66	12.19	7	0.03
07/01/80	06:43:51.31	37N36.73	118W52.38	3.83	8	0.09
07/01/80	14:25:12.33	37N36.28	118W55.30	3.96	8	0.09
07/02/80	04:13:52.79	37N31.08	118W50.73	4.23	9	0.05
07/03/80	02:39:55.93	37N37.63	118W56.74	6.84	9	0.07
07/03/80	02:41:30.58	37N38.12	118W62.24	9.63	7	0.10
07/03/80	03:31:17.29	37N29.35	118W48.62	8.73	9	0.04
07/03/80	05:55:22.23	37N37.40	118W56.81	2.85	9	0.10
07/03/80	06:00:22.01	37N37.46	118W57.25	0.91	9	0.07
07/11/80	11:29:34.27	37N32.66	118W47.20	0.00	9	0.06
07/13/80	00:45:36.25	37N29.61	118W48.93	7.56	9	0.06
07/13/80	13:42:04.98	37N27.99	118W51.19	2.51	9	0.08
07/15/80	07:16:11.97	37N30.77	118W49.90	8.95	9	0.03
07/15/80	09:17:31.62	37N28.00	118W49.26	6.67	9	0.07
07/15/80	18:36:04.54	37N37.00	118W54.14	3.09	9	0.09
07/15/80	22:36:39.19	37N37.68	118W51.42	7.89	9	0.04
07/16/80	09:11:11.12	37N32.51	118W47.78	1.44	9	0.07
07/17/80	17:06:24.62	37N35.31	118W46.46	3.85	9	0.03
07/17/80	20:19:20.25	37N35.37	118W49.20	6.67	9	0.04
07/25/80	06:44:19.29	37N34.69	118W52.99	0.42	9	0.05
07/26/80	11:22:11.20	37N29.61	118W48.55	7.00	9	0.04
07/27/80	01:33:26.82	37N35.36	118W52.45	4.87	9	0.05